JMB

Available online at www.sciencedirect.com

ScienceDirect

ELSEVIER

Retinoid Regulated Association of Transcriptional Co-regulators and the Polycomb Group Protein SUZ12 with the Retinoic Acid Response Elements of *Hoxa1*, *RARβ₂*, and *Cyp26A1* in F9 Embryonal Carcinoma Cells

Robert F. Gillespie[1] and Lorraine J. Gudas[1,2]*

[1]*Molecular Biology Program of Weill Graduate School of Medical Sciences, Cornell University, New York NY 10021, USA*

[2]*Pharmacology Department of Weill Medical College of Cornell University, New York NY 10021, USA*

*Corresponding author

Hox gene expression is activated by all-*trans* retinoic acid (RA), through binding to retinoic acid receptor-retinoid X receptor (RAR-RXR) heterodimers bound at RA response elements (RAREs) of target genes. The RARs and RXRs each have three isotypes (α, β, and γ), which are encoded by distinct genes. Hox genes are also repressed by polycomb group proteins (PcG), though how these proteins are targeted is unclear. We used chromatin immunoprecipitation assays to investigate the association of RXRα, RARγ, cofactors, and the PcG protein SUZ12 with the *Hoxa1*, *RARβ2*, and *Cyp26A1* RAREs in F9 embryonal carcinoma cells (teratocarcinoma stem cells) during RA treatment. We demonstrate that RARγ and RXRα are associated with RAREs prior to and during RA treatment. pCIP, p300, and RNA polymerase II levels increased at target RAREs upon exposure to RA. Conversely, SUZ12 was found associated with all RAREs studied and these associations were attenuated by treatment with RA. Upon RA removal, SUZ12 re-associated with RAREs. H3ac, H3K4me2, and H3K27me3 marks were simultaneously detected at target loci, indicative of a bivalent domain chromatin structure. During RA mediated differentiation, H3K27me3 levels decreased at target RAREs whereas H3ac and H3K4me2 levels remained constant. These studies provide insight into the dynamics of association of co-regulators with RAREs and demonstrate a novel link between RA signaling and PcG repression.

© 2007 Elsevier Ltd. All rights reserved.

Keywords: SUZ12; polycomb; differentiation; retinoic acid receptors; epigenetic marks

Present address: L. J. Gudas, Department of Pharmacology, Weill Medical College of Cornell University, 1300 York Ave, Room E-409, New York, NY, 10021, USA.

E-mail address of the corresponding author: ljgudas@med.cornell.edu

Introduction

Retinoic acid (RA) is an important regulator of vertebrate development and homeostasis because of its role in essential processes such as apoptosis, cell differentiation, and proliferation.[1,2] The effects of RA are mediated through binding to the retinoic acid receptors (RARs), which are members of the nuclear receptor (NR) super family.[3] There are three different RARs: RARα (NR1B1), RARβ (NR1B2) and RARγ (NR1B3), which are expressed in most cell types.[4] Members of the NR superfamily are DNA binding transcription factors whose capacity to regulate transcription is modulated by the binding of specific ligands.[4–7] RARs and other receptors for non-steroidal hormones, such as vitamin D receptor (VDR) and thyroid hormone receptor (TR), bind as

heterodimers with one of the retinoid X receptors to hormone response elements (HRE) within the regulatory elements of target genes. In contrast, the receptors for steroid hormones, which include the estrogen (ER), androgen (AR), progesterone (PR), and glucocorticoid (GR) receptors, bind as homodimers to their respective HREs.[3]

In the absence of ligand, RAR-RXR heterodimers are thought to associate with RAREs and actively repress transcription through association with the co-repressors (CoR) NCoR or SMRT.[7–9] These two proteins are found in repressor complexes containing the histone deacetylase (HDAC) HDAC3.[10,11] HDACs can deacetylate lysine residues of the N-terminal tails of histone proteins.[12] A loss of acetylation on histone tails prevents transcription through formation of a more condensed nucleosomal structure,[13] as well as reducing the affinity of co-activators that bind to histone tails through bromodomains.[14] Upon binding of the physiological agonist RA, RAR-RXR heterodimers undergo a conformational change resulting in the release of co-repressor complexes.[3] Subsequently, RAR-RXR heterodimers can associate with co-activators,[15] such as the steroid receptor co-activators (p160s),[16] the histone acetyl transferase (HAT) p300/CBP,[4] and others. Histone modifications mediated by these co-activators can create binding sites for chromatin modifiers containing specialized bromodomains.[17,18] Many ATP-dependent chromatin remodelers (SWI/SNF) which use the energy of ATP hydrolysis to reposition nucleosomes contain bromodomains, and thus can be targeted to marked nucleosomes.[19] Acetylation of specific histone residues[20] and chromatin remodeling results in the decondensation of the chromatin fiber, which is then more amenable for the recruitment of RNA polymerase II and a host of other proteins required for RA mediated transcription.[21,22] Recently it has been demonstrated that the enzymes topoisomerase II (TopoIIβ) and poly (ADP-ribose) polymerase 1 (PARP-1) are required to form a double-stranded break promoter intermediate at a RA target gene (RARβ) in order for RAR mediated transcription to occur.[23] Additionally, PARP-1 is required for the displacement of components of the transcriptional machinery prior to the initiation of RARβ transcription.[24]

Expression of the homeobox (Hox) proteins that regulate embryonic patterning and organogenesis[25] can be activated in embryonal carcinoma cells (EC) and embryonic stem (ES) cells by RA.[26,27] Retinoic acid response elements (RARE) have been identified in the enhancers of a number of Hox genes.[26,28,29] Hox gene expression is also negatively regulated by polycomb group proteins (PcG),[30] though the mechanism by which PcG proteins are recruited to Hox genes is as yet undetermined. Biochemical and genetic studies indicate that PcG proteins exist in at least two separate protein complexes: polycomb repressive complex 2/3 (PRC2) and polycomb repressive complex 1 (PRC1).[30,31] PRC2/3 is thought to be involved in the initiation of gene silencing, whereas PRC1 is implicated in the stable maintenance of gene repression. SUZ12 is a component of the PRC2/3 complex and

the expression of SUZ12 mRNA and is up-regulated in tumors of the colon, breast, and liver.[32] Additionally, the PRC2 complex contains the histone methyltransferase EZH2, which can trimethylate lysine 27 (K27) of histone H3 (H3K27me3).[33] Methylation of H3K27 *in vitro* increases binding of the chromodomain protein polycomb (Pc) to the chromatin.[33–35] Therefore it is thought that H3K27 trimethylation serves as a binding site for recruitment of PRC1.

Chromatin immunoprecipitation assays (ChIP) have been used extensively in studies monitoring the dynamics by which various NRs (most notably ER) and cofactors are recruited to regulatory elements in response to ligand.[36–38] However, there have been only limited studies pertaining to the dynamics of transcription complex assembly on RAREs in response to RA[19,24,39] and much of this work was done *in vitro* with reconstituted chromatin templates. Therefore, we initiated experiments to monitor the association dynamics of RAR-RXR heterodimers and cofactors to RAREs in F9 EC cells during RA treatment. In particular we addressed the question of whether RAR-RXR heterodimers associate with RAREs in the absence of ligand. Additionally we monitored the kinetics with which co-activators are recruited to regulatory regions in response to RA. We also monitored histone modifications (e.g. acetylation and methylation) that are usually associated with transcriptional activation at these RAREs during RA treatment. Finally, the observation that Hox genes are regulated by both RA and PcG proteins prompted us to investigate whether PcG proteins associate with RA regulatory elements, and what effect RA may have on this association.

Results

Hoxa1, *Cyp26A1*, and *RARβ2* mRNAs are induced with similar kinetics in RA-treated F9 cells

We selected the F9 EC cell line as a model system to study all-*trans*-retinoic acid (RA) mediated transcriptional regulation. F9 cells respond to RA treatment by differentiating into primitive endoderm.[3,40] We focused our studies on the regulation of the *Hoxa1*, *Cyp26*, and *RARβ2* genes, since these three genes are transcriptionally activated by RA *via* well characterized RAREs.[26,41–43] Wild-type F9 cells were treated with 1 μM RA for various times and RNA was harvested. Expression of the selected target genes was monitored by semi-quantitative RT-PCR. The *Hoxa1*, *Cyp26A1*, and *RARβ2* genes were strongly induced with similar kinetics by RA (Figure 1(a)). Expression of the three target genes could be detected within 2 h after RA addition and expression levels continued to increase over 12 to 24 h. To ensure that equivalent amounts of RNA from each time point were used in the real time (RT)-PCR assays, expression of the ribosomal phosphoprotein 36B4 "housekeeping gene"[44] was monitored, and was

(a)   Semi-quantitative RT-PCR
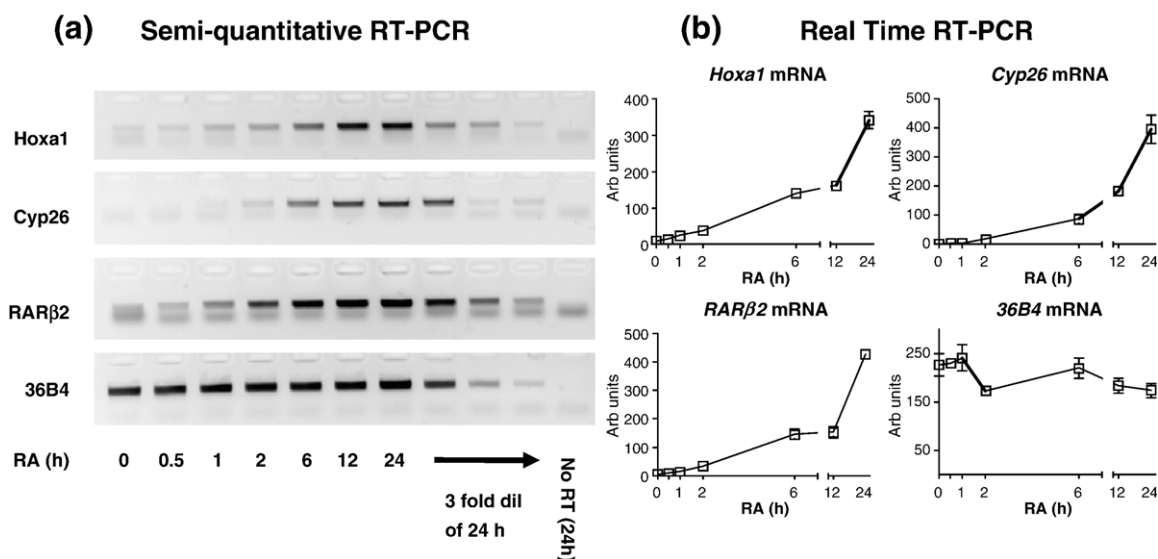
(b)   Real Time RT-PCR

Figure 1. Induction of RA target genes in F9 cells as measured by RT-PCR. (a) F9 cells were treated with RA for the indicated times and RNA was harvested. Harvested RNA was assayed by semi-quantitative RT-PCR. Each experiment was repeated at least three times; data shown are from one experiment. Linearity of the PCR reaction was demonstrated by serial dilution of the 24 h time point template. Products were visualized by standard gel electrophoresis. (b) Quantitation of RT-PCR products by real time PCR. Results depict the mean of three independent experiments (±SE) with each quantitative PCR performed in triplicate. The *y*-axis of each graph has a different scale.

shown not to fluctuate in response to RA treatment (Figure 1(a)).

The semi-quantitative RT-PCR results were confirmed and quantitated by real time PCR analysis (Figure 1(b)). All three RA target genes were induced by greater than threefold following two hours treatment with RA (Figure 1(b)). A greater than 28-fold induction were seen for each of the RA target genes after treatment of the F9 cells with 1 µM RA for 24 h. RT-PCR results confirmed that the 36B4 mRNA levels did not significantly change during the RA time course treatment (Figure 1(b)).

RARγ and RXRα are associated with RAREs in F9 cells prior to and during RA treatment

The currently accepted model of gene regulation by nuclear receptors posits that RAR-RXR heterodimers associate with RAREs in the absence of ligand, and actively repress transcription through recruitment of co-repressors such as NcoR and SMRT.[3,8] As such it is thought that RAR-RXR heterodimers are constitutively associated with RAREs and that this association is not affected by exposure to ligand. We tested this hypothesis by utilizing a two-step chromatin immunoprecipitation (ChIP) assay to monitor the association of RARγ and RXRα with RAREs in F9 cells prior to and during RA treatment. We were unable to detect association of RARγ with target RAREs using standard ChIP assays and thus utilized a recently described, more sensitive two-step cross-linking protocol.[45] Cells were cultured in the presence or absence of RA for various times and then subjected to the protein–protein cross-linking reagent disuccinimidyl glutarate (DSG). Cells were then formaldehyde-fixed as

in conventional ChIP assays, and soluble chromatin was prepared as described. Antibodies to RARγ and RXRα were used to immunoprecipitate protein–DNA complexes from soluble chromatin. Nonspecific rabbit IgG antibodies were also used as a negative control in the two-step ChIP assays.

We specifically monitored the association of RARγ and RXRα with the Hoxa1[26] and RARβ2[46] RAREs, as well as the two RAREs known to regulate expression of Cyp26. The Hoxa1 RARE is located ~2 kb downstream of the Hoxa1 gene, whereas the RARβ2 RARE is located ~55 bp upstream of the transcription start site (Figure 2(a)). Cyp26 contains a RARE ~70 bp upstream of the transcription start site denoted as R1[42] as well as a more recently described RARE denoted as R2,[43] found ~1950 bp upstream of R1 (Figure 2(a)). Additionally, we monitored RARγ-RXRα association with the promoter proximal region of the Hoxa1 gene (PP) (Figure 2(a)). The specificity of the RARγ antisera was demonstrated by Western blot and immunoprecipitation (IP) analysis (Figure 2(b) and (c)). To our knowledge, our study is the first to monitor the specific association of the RARγ isotype with RAREs in living cells. As a control for the non-specific immunoprecipitation of DNA in ChIP assays, we also measured a gene-free region located −18 kb downstream of the Hoxb1 gene (−18 kb Hoxb1). Non-specific IgG controls were also performed (Figure 2(d)). Levels of the aforementioned loci recovered in ChIP assays were quantitated by RT-PCR assays. We define fold enrichment as the percentage input of a specific locus in an IP divided by the percentage input of the Hoxb1 −18 kb 3′ negative control region in the same IP (Figure 2(d)).

RARγ and RXRα were found associated with the Hoxa1 RARE, irrespective of the presence of RA

(Figure 2(d)). In ChIP assays utilizing soluble chromatin prepared from untreated F9 cells, a ~19.6-fold enrichment of the Hoxa1 RARE was observed in RXRα IPs compared to a ~1.6-fold enrichment found in IPs utilizing non-specific IgG (Figure 2(d), upper left hand panel, 0 h). Additionally we observed an ~8.8-fold enrichment of the Hoxa1 RARE in RARγ IPs utilizing the same soluble chromatin. The association of RXRα with the Hoxa1 RARE was not affected by the presence of RA, since enrichment levels remained relatively constant during RA treatment (Figure 2(d), upper left hand panel). Levels of RARγ at the Hoxa1 RARE increased as a result of RA treatment (Figure 2(d), upper left hand panel, compare 0 h to 2 h and 6h; p value < 0.05). In contrast, RARγ and RXRα did not associate with the Hoxa1 PP region, since the enrichment levels of this locus, in RARγ and RXRα IPs, were similar to the enrichment
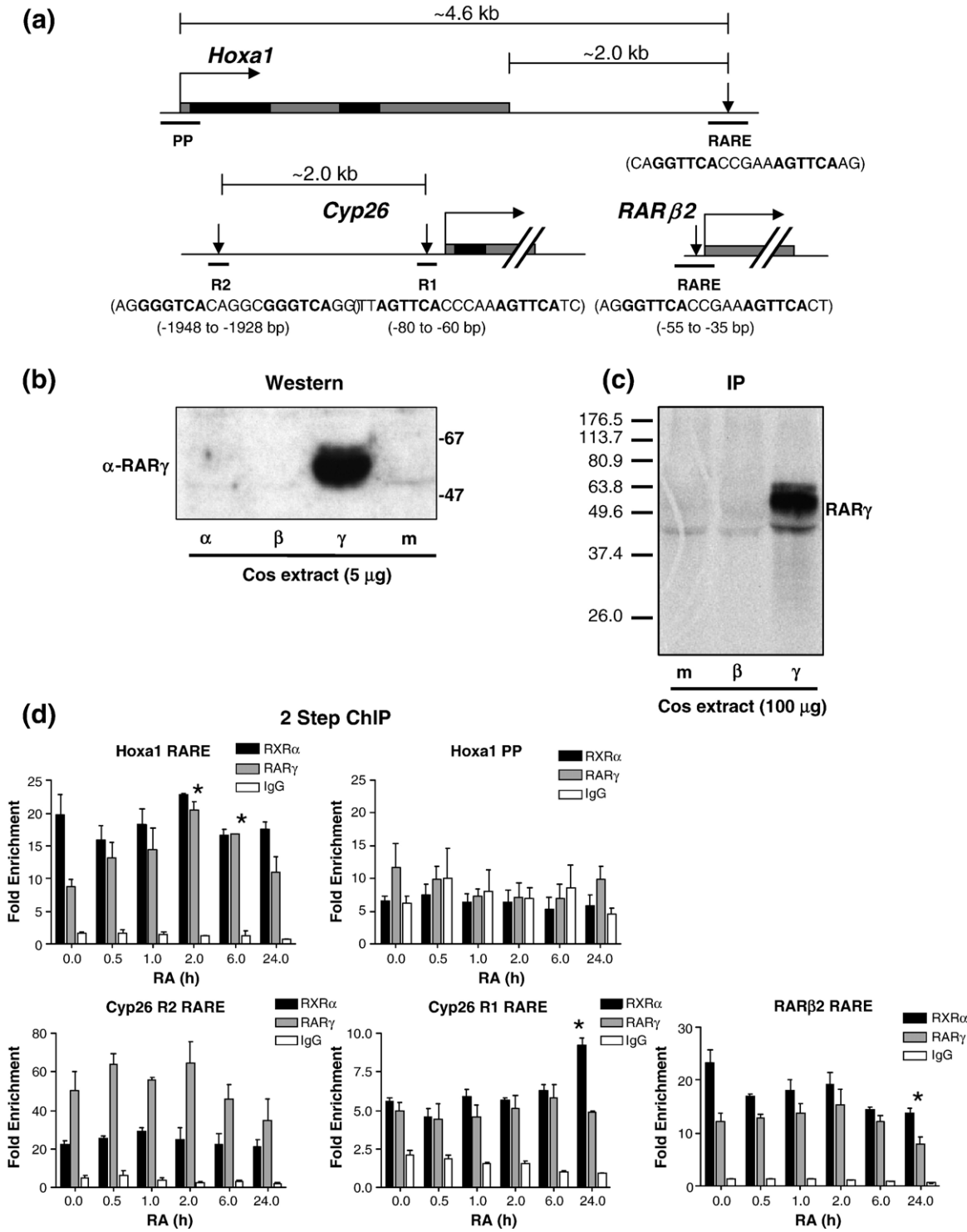

Figure 2 (*legend on next page*)

levels observed in the non-specific IgG IPs (Figure 2(d), upper middle panel).

RARγ and RXRα were also associated with both the Cyp26 R1 and R2 RAREs in F9 cells prior to treatment with RA (Figure 2(d), 0 h). For Cyp26, the levels of RARγ and RXRα were higher at the R2 RARE compared to the R1 RARE at all time points tested. For example, there was a ∼22-fold enrichment of the R2 RARE in RXRα IPs at 0 h compared to a ∼5.5-fold enrichment of the R1 RARE in these same IPs (Figure 2(d), lower panels, 0 h). These results are consistent with a recent report demonstrating that the R2 RARE mediated higher levels of RA inducibility than the R1 RARE in transient transfection assays.[43] Treatment of F9 cells with RA did not change the association levels of RXRα or RARγ with the Cyp26 RAREs (Figure 2(d), lower panels). Higher enrichment levels were observed for RARγ than RXRα at the Cyp26 R2 RARE at all time points.

RARγ and RXRα were associated with the RARβ2 RARE prior to RA treatment (Figure 2(d), bottom right hand panel, 0 h). Our results at the RARβ2 RARE are consistent with a recent report in which RAR was found constitutively bound to the RARβ2 promoter in RA treated mouse EC P19 cells.[24] Again we did not observe RA-dependent changes in the association levels of RARγ with the RARβ2 RARE. However, the levels of RXRα at the RARβ2 RARE decreased during RA treatment (Figure 2(d), compare 0 h to 24 h). From the results shown in Figure 2, we conclude that RARγ and RXRα associate with RAREs prior to and during RA treatment.

The co-activators p300 and pCIP are recruited similarly to RAREs during RA treatment of F9 cells

We next examined the kinetics of RA stimulated cofactor recruitment to RAREs through use of conventional 1 step ChIP assays. Specifically, we followed the association of the p160 co-activator pCIP,[16] as well as the histone acetyltransferase p300,[4] to RAREs during RA treatment of F9 cells. Prior to addition of RA, low levels of pCIP were associated with the Hoxa1 RARE, as there was a ∼2.2-fold enrichment of the Hoxa1 RARE relative to the −18 kb Hoxb1 negative control locus (Figure 3(a), upper left hand panel, 0 h). After 2 h of RA treatment there was a 20.5-fold enrichment of pCIP at the Hoxa1 RARE relative to the −18 kb Hoxb1 negative control locus. As expected, levels of the −18 kb Hoxb1 "negative control" locus did not increase in ChIP assays as a result of RA treatment (Figure 3). Additionally, in ChIP assays utilizing non-specific rabbit IgG, amounts of test loci immunoprecipitated were similar to the amount of the Hoxb1 −18 kb negative control region immunoprecipitated at all time points tested (data not shown in Figure 3, see Figure 4(b)). No increases in pCIP levels were seen at the Hoxa1 PP region (Figure 3(a)), indicating that the co-activator pCIP is specifically recruited to and exerts its effects from the downstream Hoxa1 enhancer.

The kinetics of pCIP recruitment to the Cyp26 RARE was similar to those seen at the Hoxa1 RARE, although the fold enrichment (relative to the Hoxb1 −18 kb negative control locus) and induction (changes in fold enrichment from time 0) were not as large at the Cyp26 RARE (Figure 3(a); 6.1 enrichment at 2 h). The Cyp26 R2 RARE was characterized[43] during the preparation of the manuscript; therefore, we only monitored co-activator recruitment to the Cyp26 R1 RARE in this study. Higher basal levels of pCIP were present at the RARβ2 RARE (Figure 3(a)) relative to those seen at the Hoxa1 and Cyp26 RAREs, and an additional ∼2.4-fold increase in pCIP levels at the RARβ2 RARE (Figure 3(a); 2 h) was observed after 2 h RA treatment. This result is consistent with a previous re-

Figure 2. Association of RARγ and RXRα with RAREs in F9 cells during RA treatment. (a) Diagram of loci monitored in ChIP assays in relation to respective transcription start sites. DNA is represented by the thin black line. Grey boxes denote regions of DNA transcribed into mRNA, whereas black boxes refer to regions of mRNA spliced and translated. The locations of the RAREs are indicated by downward pointing arrows, and the actual RARE sequences are shown directly below the arrows, with bold letters denoting binding sites. Bent arrows indicate transcription start sites, whereas hatch marks signify exon/intron gene architecture, which is not detailed. Thick black lines indicate regions of DNA amplified during ChIP assays. Schematics were drawn approximately to scale. (b) Demonstration of the specificity of the anti-RARγ antibody. Whole cell extracts (WCE) were prepared from Cos cells that were either mock transfected (m), or transfected with a plasmid expressing RARα (α), RARβ (β), or RARγ (γ). Five μg of each of the Cos WCEs were run on a SDS–12% PAGE gel followed by Western blot analysis. Anti-RARγ blue eluate was used at a 1:200 dilution to detect RARγ. The experiment was performed three times. (c) Immunoprecipitation analysis also confirms specificity of the RARγ antisera. Cos cells that were either mock transfected (m), or transfected with a plasmid expressing RARβ (β), or RARγ (γ) were metabolically labeled with [35S]methionine. Cell extracts were prepared from these cells and used in IPs with the RARγ antisera. (d) F9 cells were treated with RA for various times, then cells were fixed with DSG and formaldehyde and processed into soluble chromatin. Chromatin samples were IPed with antibodies to RARγ, RXRα, or IgG and bound DNA was quantitated by real time PCR. Fold enrichment is defined as % input of a specific loci in an IP divided by the % input of the Hoxb1 −18 kb 3′ negative control region in the same IP. Each experiment was repeated at least three times, and the quantitative PCR analyses were performed in triplicate for each sample. The data are presented as percentages of input DNA before immunoprecipitation (mean±SE). Statistical analyses were performed with Graphpad Prism 4.0. An asterisk (*) denotes a statistical significant difference ($p < 0.05$) between a time point relative to the time 0 sample for the same antibody. There were statistically significant differences ($p < 0.05$) between all RARγ IPs and the non-specific IgG negative controls, as well as between all RXRα IPs and the IgG negative controls at all of the RAREs assayed, whereas there was no statistically significant ($p > 0.05$) difference observed between both RARγ and RXRα relative to the IgG negative control at the Hoxa1 PP.

1 Step ChIP

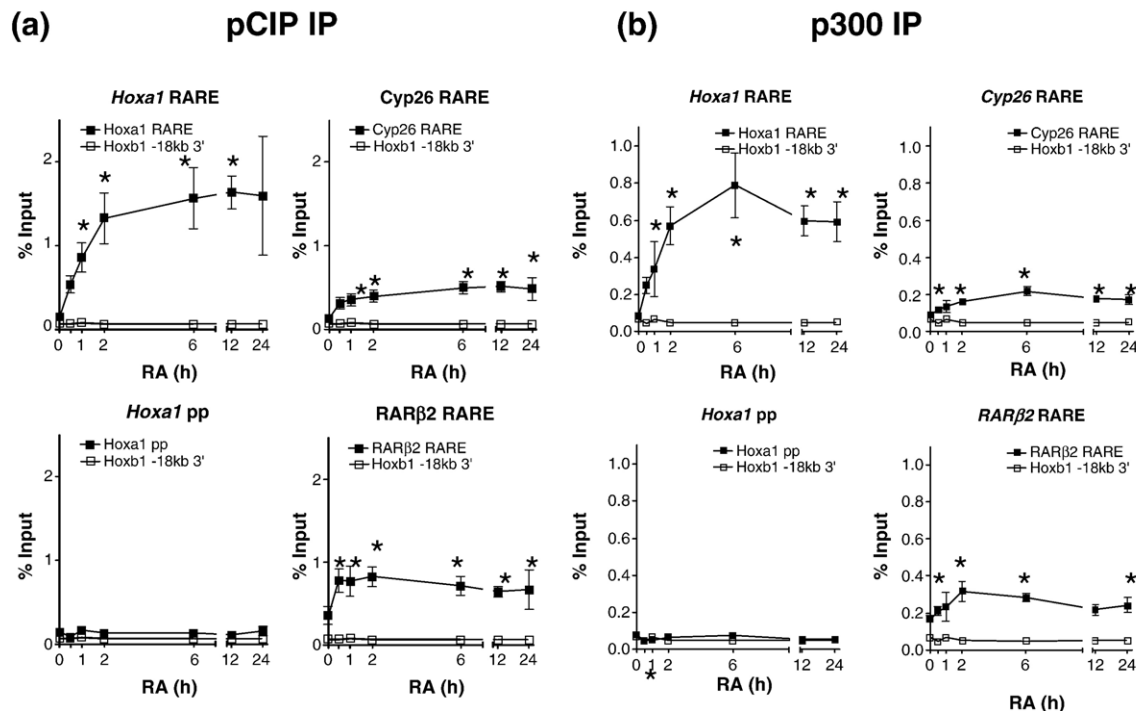**(a)** pCIP IP

(b) p300 IP

Figure 3. Recruitment of pCIP and p300 to RAREs in F9 cells during RA treatment. F9 cells were treated with RA for various times. Cells were then fixed with formaldehyde and processed into soluble chromatin. Chromatin samples were immunoprecipitated with (a) anti-pCIP antibody or (b) anti-p300 antibody, and bound DNA was quantitated by real time PCR. For comparison each target locus was graphed with the *Hoxb1* −18 kb 3′ negative control locus. Each experiment was repeated at least three times, and the quantitative PCR analyses were performed in triplicate for each sample. The data are presented as percentages of input DNA before immunoprecipitation (mean±SE). Statistical analyses were performed with Graphpad Prism 4.0. Samples that were statistically ($p < 0.05$) different from time 0 samples were denoted with an asterisk (*).

port[24] which demonstrated that much of the transcriptional machinery is associated with the *RARβ2* RARE in P19 EC cells prior to RA treatment.

The kinetics of RA mediated recruitment of the HAT p300 to RAREs monitored in this study were similar to the results seen for pCIP. Levels of p300 at the *Hoxa1* RARE rose ~9.4-fold after 2 h treatment with RA (Figure 3(b)). As was the case for pCIP, p300 did not associate with the *Hoxa1* PP region at any point during the time course (Figure 3(b)). Additionally, like pCIP, p300 levels rose over time in a RA dependent manner at the *Cyp26* RARE, though not to the extent observed at the *Hoxa1* RARE (Figure 3(b); ~3.4-fold induction at 6 h). High basal levels of p300 were found at the *RARβ2* RARE (Figure 3(b); ~2.5-fold enrichment at 0 h), and p300 levels increased ~2.5-fold (Figure 3(b); 2 h) during RA treatment. From these results we conclude that the patterns of RA mediated recruitment of pCIP and p300 to the RAREs we tested were similar.

Association of RNA polymerase II with RAREs during treatment of F9 cells with RA

We monitored the association of RNA polymerase II (pol II) with RAREs by using an antibody that

recognizes phosphorylated serine 5 of the carboxy-terminal domain (CTD) of pol II.[47] In other systems, serine 5 phosphorylation of the CTD has been associated with transcriptional initiation.[48] In the absence of RA low levels of pol II were found associated with the *Hoxa1* RARE (Figure 4(a); 0 h). After 6 h of RA treatment, pol II levels rose ~9.7-fold at the *Hoxa1* RARE (Figure 4(a)), similar to the changes shown in Figure 3 for pCIP and p300. In contrast to pCIP and p300, pol II was found associated at the *Hoxa1* PP (Figure 4(a)) in the absence of RA, with levels increasing about threefold over time as a result of RA treatment (Figure 4(a)). The levels of enrichment for pol II at the Hoxa1 PP over the Hoxb1 −18 kb negative control region were higher than for pol II at the *Hoxa1* RARE at all time points (Figure 4(a)). Given the qualitative and quantitative differences observed for pol II recruitment between the *Hoxa1* PP and RARE region, we conclude that, at least initially, pol II is recruited to the *Hoxa1* PP independently of the *Hoxa1* RARE.

Similar to the *Hoxa1* PP, pol II was also found associated with the *RARβ2* RARE in the absence of ligand (Figure 4(a)), as judged by a ~6.9-fold enrichment over the −18 kb *Hoxb1* negative control locus. This result is consistent with two previous
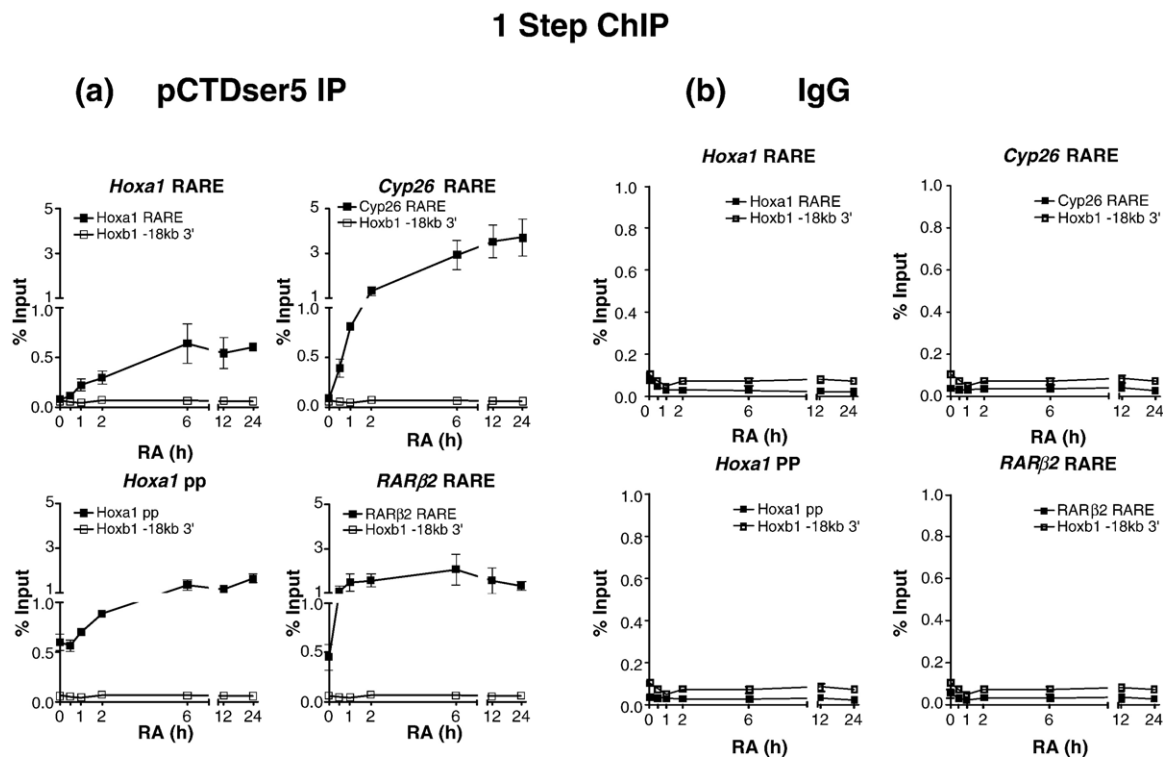
1 Step ChIP

Figure 4. Recruitment of polymerase II to RAREs in F9 cells during RA treatment. F9 cells were treated with RA for various times then cells were fixed with formaldehyde and processed into soluble chromatin. Chromatin samples were immunoprecipitated with (a) a monoclonal antibody that recognizes phosphorylated serine 5 of the CTD of RNA polymerase II or (b) non-specific rabbit IgG and bound DNA was quantitated by real time PCR. For comparison each target locus was graphed with the *Hoxb1* −18 kb 3′ negative control locus. Each experiment was repeated at least three times, and quantitative PCR analyses were performed in triplicate. The data are presented as percentages of input DNA before immunoprecipitation (mean±SE).

reports, both of which demonstrated that pol II was constitutively bound to the *RARβ2* RARE in P19 EC cells.[24,49] Polymerase II levels were increased about fivefold at the *RARβ2* RARE during the course of RA treatment (Figure 4(a); 1 h). Our results suggest that the RA signal culminating in the expression of *Hoxa1* and *RARβ2* mRNAs affects a step of the transcription process subsequent to the recruitment of pol II.

In contrast to the *Hoxa1* PP and the *RARβ2* RARE, only low levels of pol II (Figure 4(a)) were found associated with the *Cyp26* R1 RARE in the absence of ligand. Upon treatment of F9 cells with RA, a ∼47-fold increase in the levels of pol II was observed at the *Cyp26* R1 RARE. Whereas higher levels of pCIP and p300 were associated with the *Hoxa1* RARE relative to the *Cyp26* R1 RARE during RA treatment (Figure 3(a) and (b)), higher levels of pol II were found at the *Cyp26* R1 RARE compared to the *Hoxa1* RARE during RA treatment (Figure 4(a)). Finally, we note that even though the RAREs of the *Cyp26* and *RARβ2* genes are both located in close proximity to the transcription start sites (Figure 2(a)), the patterns of pol II association were markedly different for these two different RAREs. Pol II was constitutively bound at the *RARβ2* RARE, whereas very low levels of pol II were associated with the Cyp26 RARE prior to RA treatment. Additionally, the levels of pol II rose about tenfold higher at the Cyp26 RARE relative to the *RARβ2* RARE in response to RA (Figure 4(a)).

When a non-specific rabbit IgG was used in ChIP assays, the amounts of test loci immunoprecipitated were very similar to the Hoxb1 −18 kb negative control (Figure 4(b)) immunoprecipitated at all times points tested. This result demonstrates that the changes observed for enrichment levels of pCIP, p300, and pol II at our test loci during RA treatment reflected the biological response of the cells.

Acetylation and dimethylation of histone H3 do not increase at RAREs as a result of RA treatment

Active "open" chromatin suitable for transcription is often associated with histone acetylation, as well as H3 methylation at lysine 4. Thus, we conducted ChIP assays on soluble chromatin prepared from RA treated F9 cells with an antibody that recognizes acetylated lysine residue 9 (K9) and 14 (K14) of the histone H3 tail (H3K9,K14ac). Ligand-dependent increases of H3K9,K14ac have been observed for androgen, estrogen, and thyroid nuclear receptor targets genes.[37,50,51] However, in P19 EC cells, the RARβ2 RARE was found to contain constitutively high levels of H3K9,K14ac that did not further increase upon treatment with RA.[39] We also did not observe RA dependent increases in H3K9,K14ac levels at the RARβ2 RARE (Figure 5(a)). Additionally, H3K9,K14ac levels were not altered in a RA-

dependent manner at the Hoxa1 RARE or at the Hoxa1 PP region (Figure 5)(a) After 24 h of RA treatment only slight increases (less than twofold) in the levels of H3K9,K14ac relative to 0 h were seen at the Cyp26 R1 RARE (Figure 5(a)). The −18 kb Hoxb1 3′ locus was also associated with H3K9,K14ac, since higher levels of the −18 kb Hoxb1 locus were immunoprecipitated in H3K9,K14ac ChIPs relative to ChIPs with the other antibodies used in this study. For example, −18 kb Hoxb1 locus levels equivalent to ∼ 2.5% of input were immunoprecipitated in ChIP assays with the H3K9,K14ac antibody, compared to ∼ 0.06% of input pulled down in ChIP assays with the pCIP antibody.

We also conducted ChIP assays on soluble chromatin prepared from RA-treated F9 cells with an antibody that recognizes dimethylation of lysine 4 of the histone H3 tail (H3K4me2). Previous reports have demonstrated that this epigenetic histone modification is enriched at actively transcribed genes.[18,52,53] This mark has also been shown to be enriched at the promoters of androgen and estrogen target genes as the result of ligand treatment.[37,51] However, as was the case for acetylated histone H3 (Figure 5(a)), high levels of H3K4 dimethylation were detected at all of our test loci prior to RA treatment (Figure 5(b)). This result is consistent with a report demonstrating broad distribution of H3K4

dimethylation with the Hox clusters in mouse primary fibroblasts.[52] Additionally, the histone methyltransferase mixed lineage leukemia (MLL1) has been shown to bind throughout the Hox domain in U937 cells.[54] H3K4me2 levels did not increase as a result of RA treatment at any loci (Figure 5(b)). Therefore our data demonstrate that at least for the RA regulated target loci we monitored, acetylation and dimethylation of the histone H3 tails precede exposure to RA, and these levels do not change as a result of RA treatment.

SUZ12 associates with RAREs in F9 cells in the absence of RA, and this association can be attenuated by treatment with RA

Hox gene expression patterns are spatially restricted in part by the negative regulating PcG proteins.[34,55,56] We therefore investigated (a) whether PcG proteins associate with the Hoxa1 RARE and PP region and (b) whether such interactions are altered by the presence of RA. We conducted ChIP assays using an antibody that recognizes the PcG protein SUZ12. Kirimizis and colleagues[57] purified and used this antibody in ChIP assays to demonstrate an association of SUZ12 with the promoter of the MYT1 gene, as well as with other novel binding sites, in SW480 colon cancer cells. Additionally, we attempted
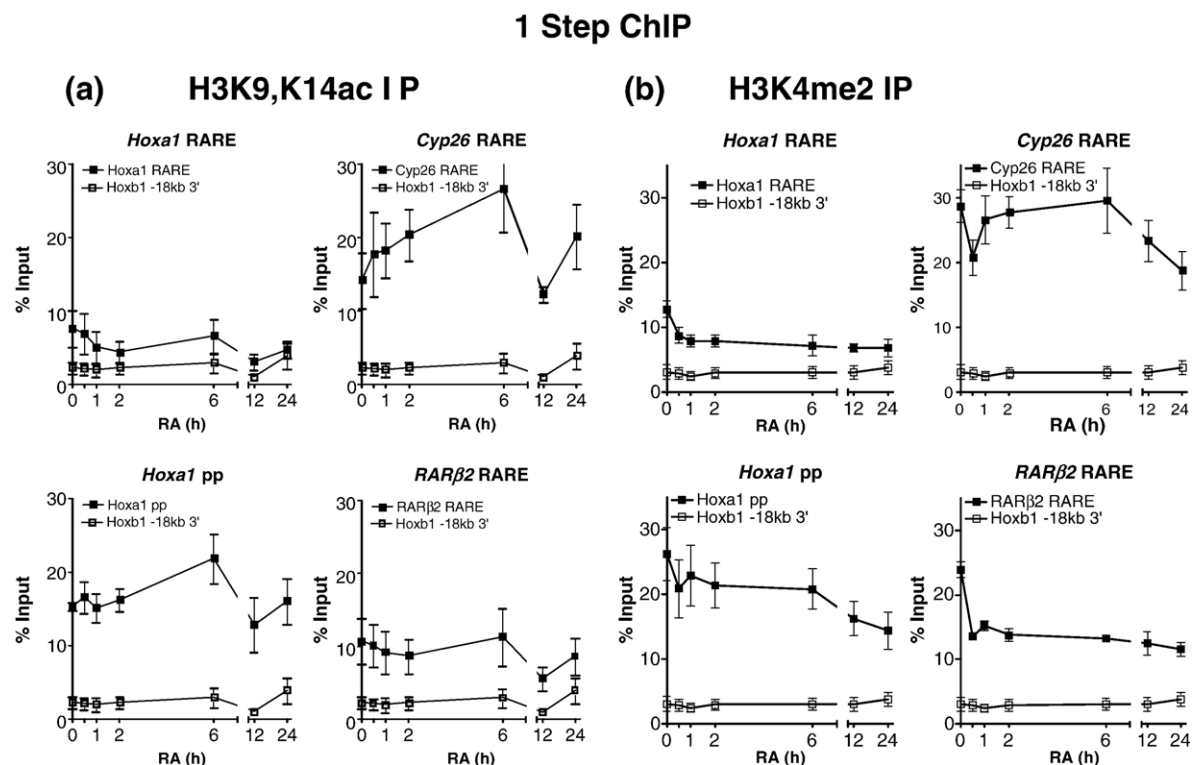

Figure 5. Acetylation and dimethylation modifications of histone H3 tails at RAREs in F9 cells do not change as a result of RA treatment. F9 cells were treated with RA for various times, and then cells were fixed with formaldehyde and processed into soluble chromatin. Chromatin samples were immunoprecipitated with (a) an anti-H3K9,K14ac antibody or (b) an anti-H3K4me2 antibody and bound DNA was quantitated by real time PCR. For comparison each target locus was graphed with the *Hoxb1* −18 kb 3′ negative control locus. Each experiment was repeated, starting with cell culture, at least three times, and the quantitative PCR analyses were performed in triplicate. The data are presented as percentages of input DNA before immunoprecipitation (mean±SE).

to conduct ChIP assays with antibodies against the PRC2/3 component EZH2 methyltranferase, but these were unsuccessful.

We did not use the −18 kb Hoxb1 region as a negative control in SUZ12 ChIP assays, since an RA-dependent decrease in levels of this locus was observed (see Discussion). Therefore, we used the Osteopontin vitamin D response element (VDRE) locus as a negative control, since osteopontin is a glycoprotein most abundantly produced in osteoblasts, and the expression of this gene is regulated by calcitropic hormones and cytokines.[58] As expected, Osteopontin expression levels in F9 cells did not change as a result of exposure to RA, as monitored by RT-PCR (data not shown). Levels of Osteopontin VDRE DNA associated with SUZ12 also remained constant during the course of RA treatment in F9 cells (Figure 6(a)).

In the absence of RA, SUZ12 was found associated with both the Hoxa1 RARE and PP region, as judged by an ~8.2-fold and a ~6.7-fold enrichment, respectively (Figure 6(a)), of these loci over the VDRE negative control locus found upstream of the Osteopontin gene.[59] Upon exposure to RA, SUZ12 levels rapidly decreased at both the Hoxa1 RARE and PP

region (Figure 6(a); from 0 h to 0.5 h). SUZ12 levels continued to decline at both these loci during the course of RA treatment (Figure 6(a)). A ~14.4-fold decrease in SUZ12 levels occurred at the Hoxa1 RARE after a 12 h treatment with RA. SUZ12 levels also decreased ~11.3-fold at the Hoxa1 PP region after exposure to RA for 12 h (Figure 6(a)). Therefore, we conclude that SUZ12 is associated with both the promoter and enhancer region of the Hoxa1 gene, and that this association is disrupted upon exposure to RA.

Having demonstrated that RA decreases the association of PcG proteins with the regulatory regions of the Hoxa1 gene, we wanted to determine if PcG proteins play a more global role in RA mediated transcriptional regulation. Therefore, we also monitored the association of SUZ12 with the Cyp26 R1 and RARβ2 RAREs during the course of RA treatment of F9 cells. Prior to RA addition, SUZ12 was found associated with the RARβ2 RARE, as judged by a ~6.4-fold enrichment of this locus over that seen for the Osteopontin VDRE (Figure 6(a)). As was the case for the Hoxa1 locus, the levels of SUZ12 at the RARβ2 RARE rapidly decreased upon exposure to RA, and after 12 h of RA treatment, SUZ12 levels at
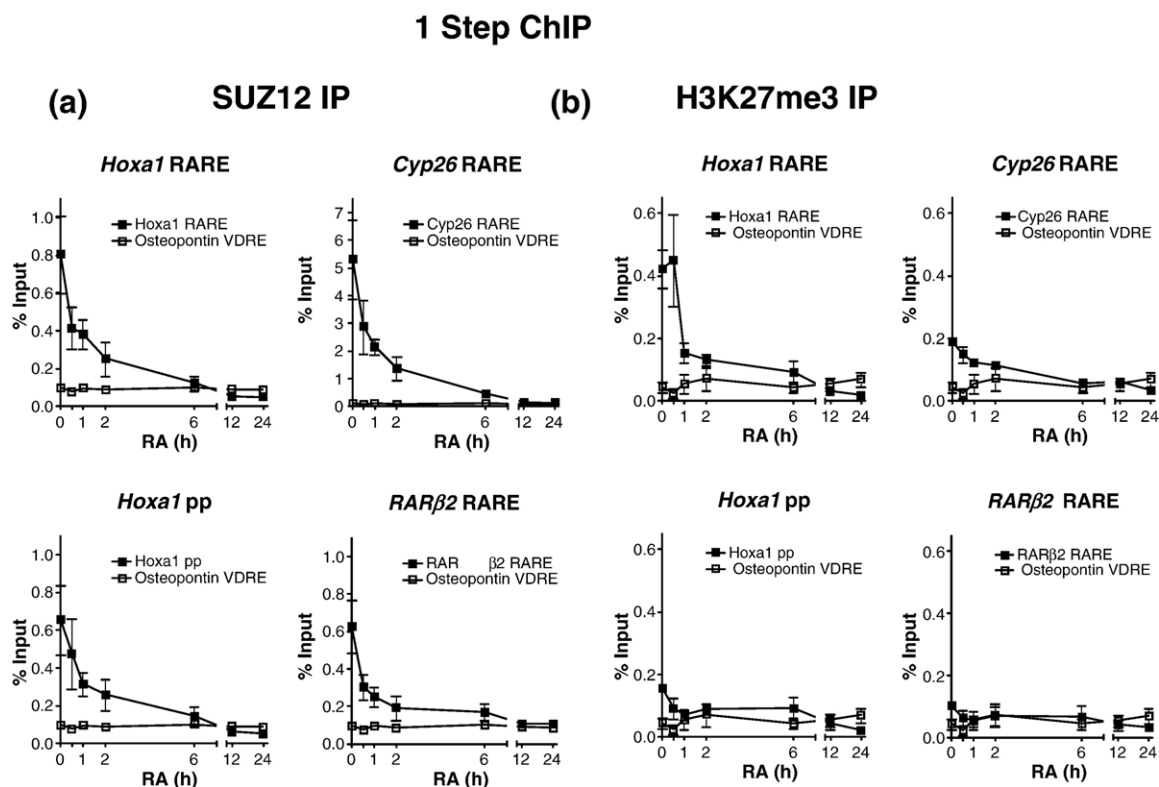

Figure 6. SUZ12 associates with RAREs in F9 cells prior to exposure to RA, and then disassociates upon RA treatment. F9 cells were treated with RA for various times. Cells were then fixed with formaldehyde and processed into soluble chromatin. Chromatin samples were immunoprecipitated with (a) an anti-SUZ12 antibody or (b) an anti-H3K27me3 antibody and bound DNA was quantitated by real time PCR. For comparison each target locus was graphed with the *Osteopontin* VDRE negative control locus. The *y*-axis of the *Cyp26* RARE graph in (a) has a different scale than the other loci graphs. Each experiment was repeated at least three times, starting with cell culture, and quantitative PCR analyses were performed in triplicate. The data are presented as percentages of input DNA before immunoprecipitation (mean±SE).

the RARβ2 RARE decreased to the background levels observed for the Osteopontin control VDRE (Figure 6(a)).

In the absence of RA, there was a ~6.6-fold higher level of SUZ12 at the Cyp26 R1 RARE relative to the Hoxa1 RARE (Figure 6(a); ~54-fold enrichment for the Cyp26 RARE at 0 h versus ~8.2-fold enrichment at 0 h for Hoxa1 RARE). Even though higher levels of SUZ12 were observed at the Cyp26 R1 RARE relative to the RARβ2 RARE and Hoxa1 regulatory regions in the absence of RA, after 12 h of RA treatment SUZ12 levels at the Cyp26 R1 RARE also decreased to the background levels observed for the Osteopontin VDRE (Figure 6(a)). The higher levels of SUZ12 initially observed at the Cyp26 R1 RARE may be inversely related to the larger increase in pol II recruitment observed at this locus as a result of RA treatment (Figure 4). That SUZ12 associated with all RAREs we tested and that this association was decreased by exposure to RA indicate that PcG proteins have a more global role in transcriptional repression of RA target genes.

Trimethylation of lysine 27 of histone H3 at RAREs also decreases in response to RA

SUZ12 has been biochemically defined as a component of the polycomb PRC2/3 complex, which also contains the histone methyltransferase EZH2.[33] PRC2/3 complexes maintain silencing in part through trimethylation of lysine 27 (H3K27me3) of histone H3.[57] If SUZ12 associates with RAREs as part of a functional PRC2/3 complex, then we would expect to observe H3K27me3 marks at the aforementioned RAREs. We conducted ChIP assays on soluble chromatin prepared from RA-treated F9 cells with a monoclonal antibody that specifically recognizes this histone H3 modification.[60] In the absence of RA, H3K27me3 was significantly higher at the Hoxa1 RARE relative to the Osteopontin control VDRE (Figure 6(b)). After 2 h exposure to RA, levels of this epigenetic mark at the Hoxa1 RARE decreased to levels observed at the Osteopontin VDRE (Figure 6(b)). H3K27me3 levels at the Cyp26 R1 RARE also decreased to background levels after exposure to RA (Figure 6(b)), though levels of this epigenetic mark were lower at the Cyp26 RARE compared to the Hoxa1 RARE. Therefore, levels of H3K27me3 at a given locus are not strictly correlated to levels of SUZ12, since we observed significantly higher levels of SUZ12 at the Cyp26 RARE relative to the Hoxa1 RARE (Figure 6(a)).

These results (Figure 6(b)) demonstrate that in the absence of RA, H3K27me3 marks, presumably mediated through the PRC2/3 complex, were present at our test RAREs. Additionally, similar to SUZ12 at these same regions, H3K27me3 levels decreased as a result of RA treatment. This latter result suggests that H3K27me3 epigenetic marks can be rapidly removed, possibly through recruitment of an unidentified demethylase capable of reversing H3K27me3 marks,[18] to RAREs upon treatment with RA. In support of this proposal, a histone demethy-

lase, lysine-specific demethylase 1 (LSD-1) has been shown to interact with a nuclear receptor (androgen) and LSD-1 is required for androgen dependent transcription.[61]

Upon removal of RA, SUZ12 re-associates with the *Cyp26* R1 RARE

We have shown that the association of SUZ12 with RA regulatory regions in F9 cells is decreased upon exposure to RA. This observation led us to ask whether SUZ12 can re-associate with a RARE in RA treated F9 cells upon removal of RA. We cultured F9 cells in the presence of RA for 24 h. After the 24 h RA treatment, media was aspirated off of cells and then these cells were rinsed three times with phosphate-buffered saline (PBS). Fresh media without RA was then added back to these cell cultures, which were then incubated for various lengths of time (0.5, 1, 6, or 24 h) prior to formaldehyde cross-linking (Figure 7(a)). Some samples were harvested immediately after the 24 h RA treatment and rinsed three times with PBS (denoted by 0, rinse in Figure 7) or were cross-linked without the PBS rinses (denoted by (0) in Figure 7) to reflect the harvesting conditions for samples in Figures 2–6. Soluble chromatin was then prepared and used in ChIP assays with antibodies to SUZ12.

Increases in SUZ12 levels at the Cyp26 R1 RARE were observed 1 h after RA removal (Figure 7(b); 1 h, ~3.2-fold induction compared to "0 (rinse)"). The level of SUZ12 continued to increase at the Cyp26 R1 RARE in response to increased times after RA removal, such that 24 h after RA removal there was a ~10.8-fold increase in the level of SUZ12 at this RARE relative to samples which were cultured in RA for 24 h and then harvested immediately after RA removal (Figure 7(b); compare 24 h to the "0 (rinse)" sample at the Cyp26 RARE). In the soluble chromatin prepared from cells that were harvested immediately after RA removal and were not rinsed immediately before cross-linking (Figure 7(b) "0"), the levels of SUZ12 at the Cyp26 RARE were similar to the levels of SUZ12 observed at the Cyp26 RARE in the "0 (rinse)" samples (Figure 7(b); compare 0 to 0 (rinse)). Additionally, soluble chromatin was prepared from F9 cells treated with RA for the entire 48 h as a positive (pos) control and from F9 cells that were cultured for 48 h without RA treatment as a negative control (neg). Higher levels of SUZ12 were observed at the Cyp26 R1 RARE in cells not treated with RA relative to cells continuously exposed to RA for 48 h (pos) (Figure 7(b); compare neg to pos), as we expected. These results show that removal of RA from F9 cells results in the re-association of SUZ12 with the Cyp26 R1 RARE.

RNA polymerase II association at RAREs decreases upon removal of RA

We have demonstrated that in F9 cells treated with RA, RNA pol II is recruited to the Cyp26 R1, on a
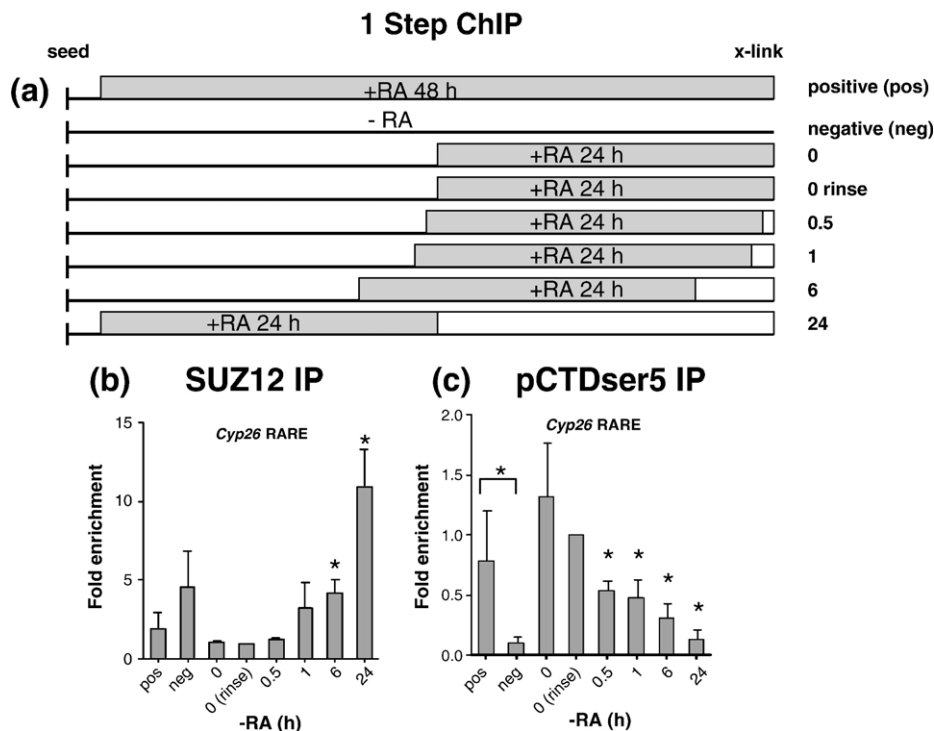
Figure 7. SUZ12 rapidly associates with RAREs whereas RNA polymerase II disassociates from RAREs upon removal of RA. (a) Schematic diagram of the RA washout ChIP experiment protocol. F9 cells were treated with RA then rinsed with PBS, and fresh media was added for various times prior to formaldehyde cross-linking and cell harvest. The time of RA addition is denoted by +RA, and the wide grey bar. The times of the PBS rinses, followed by addition of fresh media, are denoted by the change to the white bar. The positive control (pos) was treated with RA for 48 h and was not rinsed prior to cross-linking (x-link). The negative control (neg) was not treated with RA, nor rinsed prior to x-linking. The "0" sample was treated with RA for 24 h and then immediately x-linked and cells harvested. The "0 rinse" sample was rinsed three times after the 24 h RA treatment and then medium containing 1% formaldehyde was immediately added to the culture dish. The addition of RA, and the subsequent steps were staggered so that all samples were x-linked at the same time. (b) Chromatin samples were immunoprecipitated with an anti-SUZ12 antibody or (c) a monoclonal antibody that recognizes phosphorylated serine 5 of the CTD of polymerase II, and bound DNA was quantitated by real time PCR. The percent of the total input of each locus was quantitated and normalized to the negative control locus. The osteopontin VDRE was used as a negative control for SUZ12 ChIP assays, and the Hoxb1 −18 kb region was used as a negative control for pol II ChIP assays. The fold induction was then calculated relative to the 0 rinse sample. Each experiment was repeated at least three times, starting with cell culture and the quantitative PCR analyses were performed in triplicate for each experiment. The bars represent fold induction (±SE). Statistical analyses were performed with Graphpad Prism 4.0. Aa asterisk (*) denotes statistical significance ($p < 0.05$). Unless denoted otherwise, statistical significance is calculated relative to the 0 (rinse) sample.

time scale of hours (Figure 4). We have also demonstrated that upon removal of RA from F9 cells, SUZ12, presumably as part of the repressive PRC2/3 complex, is recruited to the aforementioned RARE on a similar time scale (Figure 7(b)). Therefore, we wished to determine if the recruitment of SUZ12 to the Cyp26 R1 RARE, upon removal of RA, coincided with the disassociation of pol II from the same RARE. As such, we also monitored the association of pol II with the Cyp26 R1 RARE upon removal of RA in the experiment described above. Higher levels of pol II were associated with the Cyp26 R1 RARE in F9 cells treated with RA for 48 h versus F9 cells that were not exposed to RA (Figure 7(c); compare pos to neg), consistent with the results in Figure 4. Thirty minutes after removal of RA, a decrease in pol II levels was observed at the Cyp26 R1 RARE (Figure 7(c); compare "0 rinse" to

0.5 h). Pol II levels at this RARE continued to decrease at later times after RA removal (Figure 7(c)). We conclude that upon removal of RA in F9 cells, the kinetics of pol II disassociation from the Cyp26 R1 RARE were inversely related to the kinetics of recruitment of SUZ12 to the same RAREs.

Discussion

Here we have monitored the association of RARγ, RXRα, cofactors, and histone modifications with RA regulatory elements in F9 cells before and during RA treatment. RARγ and RXRα were associated with RAREs before treatment with RA, and for the most part exposure to RA did not affect the association levels of these factors with RAREs (Figure 2). Additionally, the co-activators pCIP and p300 were

recruited to RAREs with similar kinetics during RA treatment (Figure 3). The association of RNA pol II with RA regulatory elements varied in a gene specific manner. Low levels of pol II were found at the *Hoxa1* and *Cyp26* R1 RAREs prior to RA treatment and pol II levels at these RAREs increased dramatically in response to RA treatment (Figure 4). In contrast, high levels of pol II were associated with the *RARβ2* RARE and the *Hoxa1* PP even without RA treatment (Figure 4). We also demonstrated that the levels of certain histone modifications associated with transcription (H3K9,K14ac and H3K4me2) were constitutively high at target RAREs and did not increase during RA treatment (Figure 5).

Additionally, we demonstrated that the PcG protein SUZ12 was associated with all RAREs tested in the absence of RA, and that this association was reduced by RA treatment (Figure 6(a)). Moreover, an epigenetic mark (H3K27me3), presumably mediated by the PRC 2/3 complex, was detected at our target RAREs and the H3K27me3 levels at these RAREs also decreased in response to RA (Figure 6(b)). Finally, RA treatment, followed by RA removal, resulted in SUZ12 re-association with target RAREs and a concomitant decrease in levels of pol II associated at these same RAREs (Figure 7(b) and

(c)). We have summarized the results of this study in a schematic model (Figure 8).

Association of RARγ and RXRα with RAREs

We have demonstrated that RARγ and RXRα are associated with RAREs prior to RA treatment, and that in general, association levels were not affected by the presence of RA. Consistent with our results, Pavri *et al.*[24] have also demonstrated that RAR is constitutively associated with the *RARβ2* RARE in P19 EC cells. Another recent study demonstrated that the non-steroidal thyroid hormone (TR) nuclear receptor is also constitutively associated with the TR response element (TRE) of a target gene (TRβ).[62] However in this same study, TR binding to the TRE of another target gene (TH/bZIP) was found to dramatically increase upon TR treatment. Additionally, recruitment of the non-steroidal vitamin D nuclear receptor[63] to cognate binding sites was shown to occur in a ligand-specific manner. Therefore, the question arises as to what factors determine whether a non-steroidal nuclear receptor is constitutively associated with a regulatory element. The high basal levels of acetylated and methylated (K4) histones found at RAREs (Figure 5)[39] may render RARE-
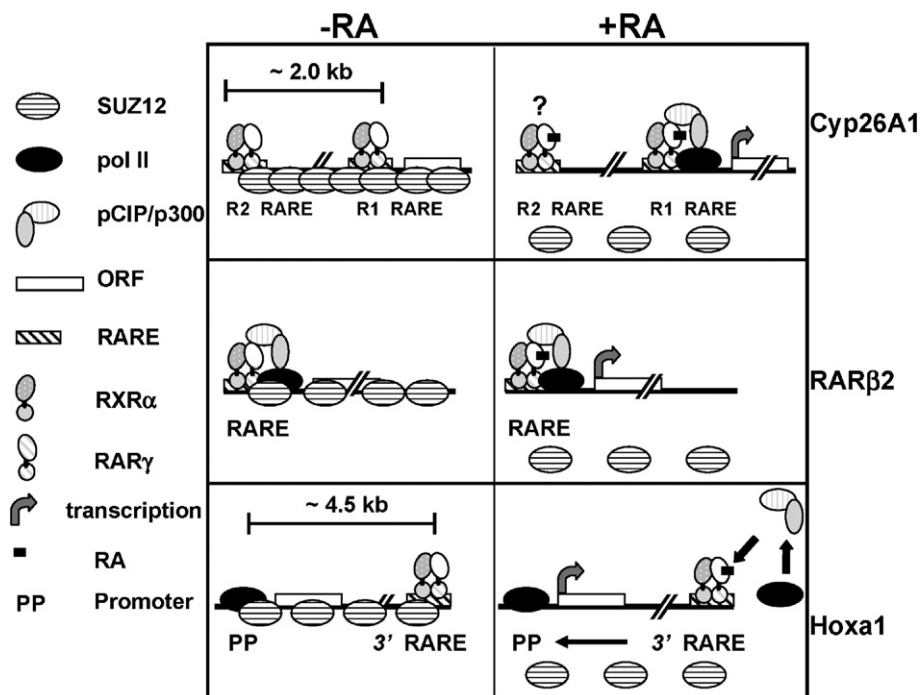

Figure 8. A model for RARγ mediated transcription of three RA target genes. In the absence of RA, RARγ-RXRα heterodimers associated with *RARβ₂*, *Hoxa1,* and *Cyp26A1* RAREs presumably repress transcription through association with co-repressors. RA target genes are also associated with SUZ12 in the absence of RA. For simplicity we have depicted SUZ12 blanketing the entire *RARβ₂* and *Cyp26A1* loci, though this has not been determined experimentally. Pol II is pre-bound to the *Hoxa1* proximal promoter (PP) and pol II, pCIP and p300 are pre-bound to the *RARβ₂* RARE. Upon ligand binding, a conformational change occurs in RARγ-RXRα heterodimers bound to RAREs. In the case of RARγ-RXRα heterodimers associated with the *Hoxa1* and *Cyp26A1* R1 RAREs, binding of RA results in the recruitment of pCIP/p300 and pol II. RA treatment also enables factors bound to the *Hoxa1* 3′ RARE to interact with the Hoxa1 PP region. Furthermore, Suz12 dissociates from the three RA target genes upon exposure to RA. Lastly, RA is required to facilitate a step subsequent to pol II recruitment at the PP regions of Hoxa1 *RARβ₂* in order for these genes to be transcribed.

containing chromatin accessible to RAR-RXR binding prior to RA treatment. As demonstrated in this study, acetylation and methylation levels were not further increased during RA treatment (Figure 5) and thus these histone modifications may be at maximal levels prior to RA treatment. Additionally, *in vitro* studies have demonstrated that histone acetylation is required for RAR-RXR binding to a nucleosomal RARE.[64] In the case of other nuclear receptors, ligand-specific increases in histone acetylation and methylation[37,51] have been reported. Thus, we speculate that the epigenetic marks associated with the chromatin embedding a hormone response element may influence the binding characteristics of the respective nuclear receptors.

Here we specifically monitored the association of RARγ and RXRα with a number of RAREs. However, there are two other isotypes of RAR (RARα, RARβ) and RXR (RXRβ, RXRγ) expressed in F9 cells.[3] It remains to be determined if RAR/RXR association with a given RARE occurs in an isotype specific manner. For example, RA induced expression of *Hoxa1* and *Cyp26* is greatly reduced in F9 RARγ −/− cells.[65] As such, RARγ may be the only RAR isotype associated with the *Hoxa1* RARE and *Cyp26* RAREs. If this is not the case, then what possible roles do RARα and RARβ have at these RAREs? Additionally, we found RARγ associated with the *RARβ2* RARE (Figure 2(b)), even though *RARβ2* expression is RA induced in F9 RARγ −/− cells.[65]

Transcriptional co-regulator levels at RAREs gradually increase during RA treatment

The recruitment dynamics of cofactors to RA regulatory elements coincided with the kinetics of RA induced expression of the *Hoxa1*, *Cyp26*, and *RARβ2* mRNAs (Figure 1). In general, co-regulators required for transcription were recruited within 2 h after RA treatment and then levels of these factors reached a plateau thereafter. We did not observe any distinct periodic cycles of transcription factor association with any of our test loci upon ligand treatment, as has been observed for androgen,[50] estrogen,[36–38,66] glucocorticoid,[67] and vitamin D receptors.[63] However, similar to the results of our study, Wang et al.[68] demonstrated that AR and cofactor levels gradually increased over a 16 h period at regulatory regions of the *PSA* gene in response to ligand, and the dynamics of AR association correlated with the kinetics of prostate specific antigen (PSA) mRNA production. The factors governing whether NRs and cofactors are recruited to promoters in discrete cycles or more progressively are unclear at this time. However, eukaryotic enhancers are modular in nature, containing binding sites for multiple transcription factors.[69,70] For example, the *Hoxa1* enhancer contains an evolutionarily conserved element (CE2) that is required for expression of *Hoxa1* in certain tissues, and is located adjacent to the *Hoxa1* RARE.[71] Thus, it is likely that the recruitment of co-regulators to regulatory elements is influenced by the binding of transcription factors to neighboring regulatory elements.

Hoxa1 RARE communication with the *Hoxa1* PP region

The *Hoxa1* RARE is located ∼ 4.6 kb downstream of the *Hoxa1* PP region (Figure 2), which raises a question about how factors bound to these two regulatory regions are able to communicate, allowing for initiation of *Hoxa1* mRNA expression. One possible explanation is that factors bound to the *Hoxa1* RARE and *Hoxa1* PP region physically interact, resulting in the folding and/or looping of the intervening DNA. If such a model were correct, then factors bound at the *Hoxa1* RARE should be brought into proximity to the *Hoxa1* PP region, and this could be observed by ChIP assays. Park *et al.*[72] used such an approach to demonstrate that TR bound to an upstream TRE became associated with a promoter proximal G/C box regulatory element in response to T₃. We have shown that RARγ, RXRα, pCIP, and p300 associated with the *Hoxa1* RARE (Figures 2 and 3) but we did not observe any of these proteins at the *Hoxa1* PP region. However, pol II was associated with both regions of the *Hoxa1* gene, and the association of pol II with the *Hoxa1* PP temporally preceded pol II association with the *Hoxa1* RARE (Figure 4). Therefore, the association of pol II with the *Hoxa1* RARE may have arisen through interaction with the *Hoxa1* PP, or alternatively, pol II may have been recruited independently to the *Hoxa1* RARE during RA treatment.

SUZ12 is associated with RAREs in F9 cells in the absence of RA

PcG proteins negatively regulate expression of *Hox* genes[34,55,56] and thus we monitored whether the PcG protein SUZ12 associates with *Hoxa1* regulatory regions. We demonstrated that SUZ12 associated with both the *Hoxa1* RARE and PP region prior to exposure to RA, and that this association decreased during RA treatment (Figure 6). Additionally, and in contrast to the other co-regulators monitored in this study, SUZ12 associated with the gene free *Hoxb1* −18 kb 3′ region (data not shown), and this association also decreased during RA treatment. During the preparation of the manuscript, studies mapping the genome wide binding sites of SUZ12 in various cell lines were published.[73–77] Consistent with our results, SUZ12 was shown to bind to large regions covering the *Hox* clusters in human ES cells,[74] as well as in *D. melanogaster* Kc cells.[77] However, for the majority of SUZ12 target genes SUZ12 is located at the transcription start site regions.[74,76]

We also demonstrated that SUZ12 associates with the *Cyp26* and *RARβ2* RAREs in the absence of RA (Figure 6). A functional role for SUZ12 in the regulation of these two genes was recently reported in the human embryonic diploid fibroblast cell line TIG3.[73] Down-regulation of SUZ12 by siRNA in this cell line resulted in the increased expression of the

Cyp26 and *RARβ2* mRNAs. The fact that SUZ12 associates with several RAREs suggests that PcG proteins have a global role in the negative regulation of RA target genes.

Chromatin structure of RA regulatory regions

We observed the simultaneous presence of histone modifications associated with transcriptional repression (H3K27me3) and activation (H3K4me2) at our target RAREs (Figures 5(b) and 6(b)). During the course of RA treatment the levels of H3K27me3 decreased whereas the levels of the H3K4me2 remained constant at these RAREs. Regions of the genome containing this "bivalent domain" chromatin structure have recently been mapped and shown to coincide with highly conserved noncoding elements (HCNEs) and/or developmental genes.[78] We also observed that H3K9, K14ac modifications found at our target RAREs remained constant during RA treatment (Figure 5(a)). This result suggests that H3K9, K14ac marks contribute to the chromatin structure found at bivalent domains. Moreover, our results raise the question as to whether or not all RA target genes are embedded in bivalent domains.

RA mediated dissociation of polycomb proteins from RA regulatory regions

While homeotic gene silencing mediated by PcG proteins is mitotically inherited during development, and thus stable in nature, we have shown that the association of PcG proteins with RA target genes can be rapidly decreased by exposure to RA (Figure 6(a)). Additionally, we showed that the epigenetic H3K27me3 mark also rapidly decreases at RAREs during RA treatment (Figure 6(b)). Our results are consistent with a recent report demonstrating that SUZ12 association with target genes was decreased during RA mediated neuronal differentiation of the human EC cell line NT2/D1.[73] We have also shown that SUZ12 can re-associate with RAREs upon removal of RA from media (Figure 7). Thus, our data indicate that association of PcG proteins with RAREs in F9 cells is the default state and that removal of PcG proteins from RAREs requires exposure to RA. How is exposure to RA mechanistically translated into the disassociation of PcG proteins from RA regulatory elements? This will be a topic for future study. Another question raised by our study is whether PcG proteins are universally associated with RARE sequences, and if so, whether PcG proteins are specifically recruited to RA target genes through RARE sequences or through some other undefined feature of these genes.

The association of PcG proteins with RA target genes may arise through interactions with RAR-RXR heterodimers. Support for such a model comes from a recent study demonstrating that the human tumor antigen PRAME (preferentially expressed antigen in melanoma) can bind to liganded RAR and repress transcription through recruitment of PcG proteins.[79] Additionally, the authors showed that stable expression of PRAME in F9 cells blocked RA induced differentiation and inhibited RA induced gene expression. In the context of wild-type F9 cells, we posit that an as yet unidentified protein may simultaneously interact with PcG proteins and RAR-RXR heterodimers in the absence of RA, allowing for the recruitment of PcG proteins to RA target genes.

We have conducted ChIP studies to monitor the dynamics of association of RARγ, RXRα, and cofactors to RA regulatory regions during treatment with RA. These studies have revealed the patterns and kinetics by which these factors are recruited to different target genes. We have also revealed a novel link between PcG silencing and RAR signaling. Our data suggest that PcG proteins can be targeted to specific areas of the genome through association with RAREs (Figure 6). Moreover, we have demonstrated that levels of SUZ12 and repressive epigenetic marks generated by the PRC 2/3 complex at RAREs can be attenuated by exposure to RA (Figure 6). Thus, our data suggest a mechanism by which PcG mediated repression of target genes may be alleviated. More specifically, the results presented herein may explain how PcG mediated repression of *Hox* gene expression is relieved during activation by treatment with RA.

Materials and Methods

Cell culture

F9 wild-type embryonal carcinoma cells were cultured in Dulbecco's modified Eagle's medium supplemented with 10% (v/v) fetal calf serum (Invitrogen), 2 mM glutamine, 100 units/ml of penicillin, and 100 μg/ml of streptomycin. Cells were plated in gelatin-coated tissue culture plates approximately 48 h prior to RNA harvesting (5×10^5 cells/60 mm dish) or formaldehyde fixation (2.5×10^6 cells/20 cm dish). Treatment with 1 μM retinoic acid for 0, 0.5, 1, 2, 6, 12, and 24 h was staggered so that all time points were collected simultaneously.

Antibodies and chemicals

All-*trans* Retinoic acid (RA) was obtained from Sigma-Aldrich (St. Louis, MO) and dissolved in ethanol. Anti-RARγ serum was generated by immunization of rabbits with a peptide corresponding to 15 amino acids at the carboxy-terminal of RARγ. Polyclonal anti-RARγ IgG was purified from the crude serum through use of a DEAE Affigel Blue Gel column (Bio-Rad, Hercules, CA). Anti-RXRα (D-20, sc-553), anti-pCIP (M-397, sc-9119), anti-p300 (N-15, sc-584) antibodies were purchased from Santa Cruz Biotechnology (Santa Cruz, CA). Anti-H3K4me2 (07-030), anti-H3K9,K14ac (06-599), and anti-SUZ12 (07-379) antibodies were purchased from Upstate Biotechnology (Lake Placid, NY). Anti-phospho Ser5 CTD of RNA polymerase II (pCTDser5) was purchased from Covance Research Products (Richmond, CA). Anti-SUZ12 (ab12201, since discontinued) and anti-H3K27me3 (mAbcam 6002) antibodies were purchased from Abcam Inc. (Cambridge, MA).

RNA preparation and RT-PCR

F9 EC cells were plated in 60 mm dishes (5×10^5 cells/dish) and treated with RA as indicated. Total RNA was prepared using Trizol reagent (Invitrogen Life Technologies, Carsbad, CA) according to the manufacturer's instructions. Reverse transcription (RT) was performed on 2 µg RNA from each timepoint using 50 ng oligo (deoxythymidine) and 50 units of Superscript II (Invitrogen Life Technologies, Carsbad, CA) reverse transcriptase as recommended by the manufacturer. Synthesized cDNAs were diluted 1:10 prior to use in semi-quantitative or real time PCR reactions. Each experiment was conducted on three independent occasions.

Western blot and immunoprecipitation analysis

Whole cell extracts (WCE) were prepared from Cos cells that were either mock transfected (m), or transfected with a plasmid expressing RARα, RARβ, or RARγ. Five µg of each of the Cos WCEs were run on a SDS–12% (w/v)PAGE gel followed by transfer to a nitrocellulose membrane (0.45 µm pore size; catalog number 162-0090; Bio-Rad Hercules, CA). The membrane was stained with Ponceau S (Sigma) to ensure proper transfer and equivalent loading. Primary antibody incubation was done overnight at 4 °C. The Anti-RARγ blue eluate, as described above, was used at a 1:200 dilution to detect RARγ. After a 1 h incubation with an immunoglobulin G horseradish peroxidase–conjugated secondary antibody at room temperature (anti-rabbit, 1:40,000 dilution; sc-2030; Santa Cruz Biotechnology), the membranes were developed with Supersignal Substrate (Pierce, Rockford, IL) for 5 min and exposed to Biomax film (Eastman Kodak, Rochester, NY). Primary and secondary antibodies were diluted in PBS containing 5% Blotto (Santa Cruz Biotechnology) and 0.1% (v/v) Tween 20. For IP analysis, Cos cells either mock-transfected or transfected with a plasmid expressing either RARγ or RARβ, were metabolically labeled with 100 µCuries of [^{35}S] methionine for 1 h. Cos cell extract was then prepared from each of these cells and 100 µg of each of the extracts were immunoprecipitated with 25 µl of RARγ blue eluate. IP complexes were isolated by incubation with 25 µl of a 50:50 (v/v) slurry of a Protein A Sepharose/TE mixture. After three washes with ChIP lysis buffer, Protein A Sepharose-IP complexes were resuspended in SDS loading buffer and ran on a SDS–12% PAGE gel. The gels were then fixed and subjected to autoradiography.

ChIP assays

For two-step chromatin immunoprecipitation (ChIP) assays, 2.5×10^6 F9 EC cells were grown in a 20 cm dish and the cells were treated with 1 µM retinoic acid as indicated. Approximately (~) 36 h after plating (~1.8×10^7 to 2.3×10^7 cells), cells were briefly rinsed with PBS, and then fixed with 10 ml of 2 mM disuccinimidyl glutarate (DSG; Pierce, Rockford IL)/PBS at room temperature with shaking for 45 min. A 0.5 M stock concentration of DSG was prepared immediately before use by dissolving powdered DSG in 100% dimethyl sulfoxide. Cells were then briefly rinsed with PBS and subsequently fixed with 10 ml of 1% (v/v) formaldehyde (J.T. Baker, Phillipsburg, NJ)/PBS at room temperature with shaking for 10 min. In one-step ChIP experiments requiring only formaldehyde fixation, cells were fixed by directly adding formaldehyde (37%) to culture media (1% final concentration) and

incubating at room temperature with shaking for 10 min. In both one and two-step ChIP assays, formaldehyde fixation was quenched by the addition of 1.25 M glycine to a 200 mM final concentration. Cells were then washed with cold phosphate buffered saline (PBS) and lysed by adding 350 µl of lysis buffer (50 mM Tris–HCl (pH 8.0), 150 mM NaCl, 5 mM EDTA, 1% (v/v) NP-40, 0.5% (w/v) sodium deoxycholate, 0.5× Complete Mini protease inhibitors, cat. no. 11836153001 (Roche Molecular Biochemicals, Mannheim, Germany)) to the cell pellet. The amount of lysis buffer added to samples was adjusted to normalize for differences in cell numbers between plates. DNA was sheared by sonicating for 2×15 s (setting 3) on a Branson 150 Sonifier, and cell debris was eliminated by centrifugation at 14,000 rpm for 10 min at 4 °C. For each immunoprecipitation (IP), 50 µl of soluble chromatin (usually out of a total volume of ~350 µl) was diluted tenfold with lysis buffer and pre-cleared with 25 µl of a 50% Protein A Sepharose/PBS slurry (cat. no. 17-0780-01 (Amersham Biosciences, Uppsla Sweden)) for 1–2 h at 4 °C.

Immunoprecipitations were performed at 4 °C overnight with 2 µg of each specific antibody. Complexes were collected by incubation with 50 µl of 50% Protein A Sepharose/PBS slurry for 2 h at 4 °C. For immunoprecipitations with anti-pCTD antibodies, 2.5 µg of anti-IgM (M8644-1MG; Sigma-Aldrich) was added 1 h prior to addition of beads. Beads were washed twice for 5 min at room temperature with lysis buffer. Two more washes were carried out with ChIP wash buffer (50 mM Tris–HCl (pH 8.5), 500 mM LiCl, 5 mM EDTA, 1% NP-40, 1% sodium deoxycholate) followed by two washes in TE buffer (10 mM Tris–HCl (pH 8.0), 1 mM EDTA). Immunocomplexes were eluted from beads by incubation with 100 µl elution buffer (50 mM Tris–HCl (pH 8.0), 1% SDS, 1 mM EDTA) at 65 °C for 10 min, followed by vortexing for 15 s. After a brief centrifugation step, eluted protein–DNA complexes were transferred to new tubes, NaCl was added to a final concentration of 200 mM, and samples were incubated at 65 °C overnight to reverse cross-linking.

DNA was purified using a Qiaquick Spin Kit (Qiagen Sciences, MD) and assayed by either real time PCR or semi-quantitative PCR. For input samples, 25 µl (5.5% of amount used for IP with specific antibody) was added to 75 µl of elution buffer, NaCl was added to a 200 mM final concentration, and reverse cross-linked at 65 °C overnight. Each ChIP experiment was carried out on at least three independent occasions, starting with cell culture.

RA washout ChIP experiments

F9 EC cells (2.5×10^6) were grown in 20 cm dishes and treated with RA for 24 h (pulse). Media were then aspirated off of plates, and the cells were rinsed with PBS three times. Fresh media lacking RA was then added back to the plates and the cultures were incubated at 37 °C for various lengths of time (chase). Treatment with RA was staggered so that all plates were cross-linked at the same time (Figure 7(a)). For example, the -RA 24 h sample was initially exposed to RA 18 h earlier than the -RA 6 h sample. Consequently the -RA 24 h sample was rinsed with PBS 18 h earlier than the -RA 6 h sample. The positive control sample was exposed to RA for 48 h, whereas the negative control did not receive treatment with RA.

Table 1. DNA sequences of oligonucleotides used for ChIP and RT-PCR

Loci	Sense primer (5′–3′)	Antisense primer (5′–3′)	Product size (bp)
A. *ChIP primers*			
Hoxa1 rare	TCTTGCTGTGACTGTGAAGTCG	GAGCTCAGATAAACTGCTGGGACT	268
Hoxa1 pp	ATTGGCTGGTAGAGTCACGTG	GAAAGTTGTAATCCCATGGTCAGA	276
CYP26 R1 rare	CCCGATCCGCAATTAAAGATGA	CTTTATAAGGCCGCCCAGGTTAC	87
CYP26 R2 rare	TTCACTGAGATGTCACGGTCC	TTCCCAATCCTTTAGCCTGA	64
RARβ2 rare	TGGCATTGTTTGCACGCTGA	CCCCCCTTTGGCAAAGAATAGA	284
−18 kb *Hoxb1* 3′	ACTCCAGCTCCCATTTCCCACTT	CTGCCTGCCTCTGCCTCACA	411
Osteopontin	GTATTCCAGTCTCACAAACTGCTTG	CATACTGTGTTCCAGGTCAGTTGG	336
B. *RT-PCR primers*			
Hoxa1[a]	TGGAGGAAGTGAGAAAGTTGGC	ATGGGAGTCGAGAGGTTTCC	484
[b]	TTCCCACTCGAGTTGTGGTCCAAGC		147
CYP26	GAAACATTGCAGATGGTGCTTCAG	CGGCTGAAGGCCTGCATAATCAC	272
RARβ2	GATCCTGGATTTCTACACCG	CACTGACGCCATAGTGGTA	247
36B4	AGAACAACCCAGCTCTGGAGAAA	ACACCCTCCAGAAAGCGAGAGT	448
Osteopontin	TGACGAATCTCACCATTCGGATGA	TTTCCAGACTTGGTTCATCCAGCT	338

[a] Primer used in semi-quantitative PCR analysis.
[b] Primer used in real time RT-PCR analysis.

Semi-quantitative and real time PCR

Semi-quantitative PCRs were performed with Taq polymerase in 20 μl reactions containing PCR buffer (final concentration of 100 mM Tris–HCl (pH 8.3), 100 mM KCl, 1.8 mM MgCl$_2$), 0.1 mM concentration of each deoxynucleoside triphosphate, 0.1 μM concentration of each primer (Table 1), and 3 μl of template. Reactions were performed in a MJ Research PTC-200 thermal cycler using a touchdown protocol as follows: following a 15 s 94 °C denaturation step, the initial annealing/extension temperature started at 70 °C (30 s) and was reduced by 0.5 °C for each of the first 20 cycles. The number of additional cycles (2–13) utilizing a 60 °C annealing/extension step (30 s) varied for each primer pair. PCR products were electrophoresed in a 2% (w/v) agarose gel and visualized with ethidium bromide (0.3 mg/ml). Amplification in the linear range was demonstrated by threefold serial dilution of templates. Real time PCR assays were carried out on a MJ Research Opticon DNA Engine using the same reaction mixture as described above, supplemented with a final concentration of 5% dimethyl sulfoxide (DMSO) and 1:20,000 dilution of SYBR green reagent (Invitrogen Life Technologies, Carsbad, CA). The touchdown protocol describe above was used for amplification with the following modifications: the initial annealing/extension step of 70 °C was decreased 1.0 °C for ten cycles, followed by an additional 35 cycles utilizing a 60 °C annealing/extension step. Fluoresence was monitored during a 5 s 77 °C step (temperature was modified depending on primer pair) immediately after the 60 °C annealing/extension steps. Real time data were quantitated through use of a standard curve generated by serial dilution of input samples. Standard curves were shown to be linear in the range of 30% to 0.001% of the input. ChIP samples were quantitated by measuring CT values and interpolating the percentage input on the standard curve. Each experiment was repeated at least three times, and quantitative PCRs were performed in triplicate. Results are presented as the mean of triplicates, along with error bars corresponding to the standard error. Statistical analyses of ChIP assays were performed by a two-way analysis of variance using the software GraphPad Prism 4.0. The UCSC *in silico* PCR program† was used to ensure primers designed for ChIP

generated a single amplicon from the appropriate target loci.

References

1. Mark, M., Ghyselinck, N. B. & Chambon, P. (2006). Function of retinoid nuclear receptors: lessons from genetic and pharmacological dissections of the retinoic acid signaling pathway during mouse embryogenesis. *Annu. Rev. Pharmacol. Toxicol.* **46**, 451–480.
2. Means, A. L. & Gudas, L. J. (1995). The roles of retinoids in vertebrate development. *Annu. Rev. Biochem.* **64**, 201–233.
3. Bastien, J. & Rochette-Egly, C. (2004). Nuclear retinoid receptors and the transcription of retinoid-target genes. *Gene*, **328**, 1–16.
4. Chambon, P. (2005). The nuclear receptor superfamily: a personal retrospect on the first two decades. *Mol. Endocrinol.* **19**, 1418–1428.
5. Gronemeyer, H., Gustafsson, J. A. & Laudet, V. (2004). Principles for modulation of the nuclear receptor superfamily. *Nature Rev. Drug Discov.* **3**, 950–964.
6. Olefsky, J. M. (2001). Nuclear receptor minireview series. *J. Biol. Chem.* **276**, 36863–36864.
7. Rochette-Egly, C. (2005). Dynamic combinatorial networks in nuclear receptor-mediated transcription. *J. Biol. Chem.* **280**, 32565–32568.
8. Glass, C. K. & Rosenfeld, M. G. (2000). The coregulator exchange in transcriptional functions of nuclear receptors. *Genes Dev.* **14**, 121–141.
9. Hartman, H. B., Yu, J., Alenghat, T., Ishizuka, T. &

† http://www.genome.ucsc.edu/cgi-bin/hgPcr

Lazar, M. A. (2005). The histone-binding code of nuclear receptor co-repressors matches the substrate specificity of histone deacetylase 3. *EMBO Rep.* **6**, 445–451.

10. Guenther, M. G., Lane, W. S., Fischle, W., Verdin, E., Lazar, M. A. & Shiekhattar, R. (2000). A core SMRT co-repressor complex containing HDAC3 and TBL1, a WD40-repeat protein linked to deafness. *Genes Dev.* **14**, 1048–1057.

11. Li, J., Wang, J., Wang, J., Nawaz, Z., Liu, J. M., Qin, J. & Wong, J. (2000). Both corepressor proteins SMRT and N-CoR exist in large protein complexes containing HDAC3. *EMBO J.* **19**, 4342–4350.

12. Grozinger, C. M. & Schreiber, S. L. (2002). Deacetylase enzymes: biological functions and the use of small-molecule inhibitors. *Chem. Biol.* **9**, 3–16.

13. Kouzarides, T. (2000). Acetylation: a regulatory modification to rival phosphorylation? *EMBO J.* **19**, 1176–1179.

14. Zeng, L. & Zhou, M. M. (2002). Bromodomain: an acetyl-lysine binding domain. *FEBS Letters*, **513**, 124–128.

15. Perissi, V. & Rosenfeld, M. G. (2005). Controlling nuclear receptors: the circular logic of cofactor cycles. *Nature Rev. Mol. Cell. Biol.* **6**, 542–554.

16. McKenna, N. J. & O'Malley, B. W. (2002). Combinatorial control of gene expression by nuclear receptors and coregulators. *Cell*, **108**, 465–474.

17. de la Cruz, X., Lois, S., Sanchez-Molina, S. & Martinez-Balbas, M. A. (2005). Do protein motifs read the histone code? *Bioessays*, **27**, 164–175.

18. Martin, C. & Zhang, Y. (2005). The diverse functions of histone lysine methylation. *Nature Rev. Mol. Cell. Biol.* **6**, 838–849.

19. Narlikar, G. J., Fan, H. Y. & Kingston, R. E. (2002). Cooperation between complexes that regulate chromatin structure and transcription. *Cell*, **108**, 475–487.

20. Shogren-Knaak, M., Ishii, H., Sun, J. M., Pazin, M. J., Davie, J. R. & Peterson, C. L. (2006). Histone H4-K16 acetylation controls chromatin structure and protein interactions. *Science*, **311**, 844–847.

21. Dilworth, F. J. & Chambon, P. (2001). Nuclear receptors coordinate the activities of chromatin remodeling complexes and coactivators to facilitate initiation of transcription. *Oncogene*, **20**, 3047–3054.

22. Rochette-Egly, C., Adam, S., Rossignol, M., Egly, J. M. & Chambon, P. (1997). Stimulation of RAR alpha activation function AF-1 through binding to the general transcription factor TFIIH and phosphorylation by CDK7. *Cell*, **90**, 97–107.

23. Ju, B. G., Lunyak, V. V., Perissi, V., Garcia-Bassets, I., Rose, D. W., Glass, C. K. & Rosenfeld, M. G. (2006). A topoisomerase IIbeta-mediated dsDNA break required for regulated transcription. *Science*, **312**, 1798–1802.

24. Pavri, R., Lewis, B., Kim, T. K., Dilworth, F. J., Erdjument-Bromage, H., Tempst, P. *et al.* (2005). PARP-1 determines specificity in a retinoid signaling pathway via direct modulation of mediator. *Mol. Cell*, **18**, 83–96.

25. Krumlauf, R. (1994). Hox genes in vertebrate development. *Cell*, **78**, 191–201.

26. Langston, A. W. & Gudas, L. J. (1992). Identification of a retinoic acid responsive enhancer 3′ of the murine homeobox gene Hox-1.6. *Mech. Dev.* **38**, 217–227.

27. LaRosa, G. J. & Gudas, L. J. (1988). Early retinoic acid-induced F9 teratocarcinoma stem cell gene ERA-1: alternate splicing creates transcripts for a homeobox-containing protein and one lacking the homeobox. *Mol. Cell. Biol.* **8**, 3906–3917.

28. Langston, A. W., Thompson, J. R. & Gudas, L. J. (1997). Retinoic acid-responsive enhancers located 3′ of the Hox A and Hox B homeobox gene clusters. Functional analysis. *J. Biol. Chem.* **272**, 2167–2175.

29. Mainguy, G., In der Rieden, P. M., Berezikov, E., Woltering, J. M., Plasterk, R. H. & Durston, A. J. (2003). A position-dependent organisation of retinoid response elements is conserved in the vertebrate Hox clusters. *Trends Genet.* **19**, 476–479.

30. Ringrose, L. & Paro, R. (2004). Epigenetic regulation of cellular memory by the Polycomb and Trithorax group proteins. *Annu. Rev. Genet.* **38**, 413–443.

31. Lund, A. H. & van Lohuizen, M. (2004). Polycomb complexes and silencing mechanisms. *Curr. Opin. Cell Biol.* **16**, 239–246.

32. Kirmizis, A., Bartley, S. M. & Farnham, P. J. (2003). Identification of the polycomb group protein SU(Z)12 as a potential molecular target for human cancer therapy. *Mol. Cancer Ther.* **2**, 113–121.

33. Cao, R. & Zhang, Y. (2004). The functions of E(Z)/EZH2-mediated methylation of lysine 27 in histone H3. *Curr. Opin. Genet. Dev.* **14**, 155–164.

34. Cao, R., Wang, L., Wang, H., Xia, L., Erdjument-Bromage, H., Tempst, P. *et al.* (2002). Role of histone H3 lysine 27 methylation in Polycomb-group silencing. *Science*, **298**, 1039–1043.

35. Czermin, B. & Imhof, A. (2003). The sounds of silence–histone deacetylation meets histone methylation. *Genetica*, **117**, 159–164.

36. Metivier, R., Penot, G., Carmouche, R. P., Hubner, M. R., Reid, G., Denger, S. *et al.* (2004). Transcriptional complexes engaged by apo-estrogen receptor-alpha isoforms have divergent outcomes. *EMBO J.* **23**, 3653–3666.

37. Metivier, R., Penot, G., Hubner, M. R., Reid, G., Brand, H., Kos, M. & Gannon, F. (2003). Estrogen receptor-alpha directs ordered, cyclical, and combinatorial recruitment of cofactors on a natural target promoter. *Cell*, **115**, 751–763.

38. Shang, Y., Hu, X., DiRenzo, J., Lazar, M. A. & Brown, M. (2000). Cofactor dynamics and sufficiency in estrogen receptor-regulated transcription. *Cell*, **103**, 843–852.

39. Lefebvre, B., Ozato, K. & Lefebvre, P. (2002). Phosphorylation of histone H3 is functionally linked to retinoic acid receptor beta promoter activation. *EMBO Rep.* **3**, 335–340.

40. Wang, S. Y., LaRosa, G. J. & Gudas, L. J. (1985). Molecular cloning of gene sequences transcriptionally regulated by retinoic acid and dibutyryl cyclic AMP in cultured mouse teratocarcinoma cells. *Dev. Biol.* **107**, 75–86.

41. de The, H., Vivanco-Ruiz, M. M., Tiollais, P., Stunnenberg, H. & Dejean, A. (1990). Identification of a retinoic acid responsive element in the retinoic acid receptor beta gene. *Nature*, **343**, 177–180.

42. Loudig, O., Babichuk, C., White, J., Abu-Abed, S., Mueller, C. & Petkovich, M. (2000). Cytochrome P450RAI(CYP26) promoter: a distinct composite retinoic acid response element underlies the complex regulation of retinoic acid metabolism. *Mol. Endocrinol.* **14**, 1483–1497.

43. Loudig, O., Maclean, G. A., Dore, N. L., Luu, L. & Petkovich, M. (2005). Transcriptional co-operativity between distant retinoic acid response elements in regulation of Cyp26A1 inducibility. *Biochem. J.* **392**, 241–248.

44. Chiba, H., Clifford, J., Metzger, D. & Chambon, P. (1997). Specific and redundant functions of retinoid X

Receptor/Retinoic acid receptor heterodimers in differentiation, proliferation, and apoptosis of F9 embryonal carcinoma cells. *J. Cell Biol.* **139**, 735–747.

45. Nowak, D. E., Tian, B. & Brasier, A. R. (2005). Two-step cross-linking method for identification of NF-kappaB gene network by chromatin immunoprecipitation. *Biotechniques*, **39**, 715–725.

46. Sucov, H. M., Murakami, K. K. & Evans, R. M. (1990). Characterization of an autoregulated response element in the mouse retinoic acid receptor type beta gene. *Proc. Natl Acad. Sci. USA*, **87**, 5392–5396.

47. Espinosa, J. M., Verdun, R. E. & Emerson, B. M. (2003). p53 functions through stress- and promoter-specific recruitment of transcription initiation components before and after DNA damage. *Mol. Cell*, **12**, 1015–1027.

48. Palancade, B. & Bensaude, O. (2003). Investigating RNA polymerase II carboxyl-terminal domain (CTD) phosphorylation. *Eur. J. Biochem.* **270**, 3859–3870.

49. Lefebvre, B., Brand, C., Lefebvre, P. & Ozato, K. (2002). Chromosomal integration of retinoic acid response elements prevents cooperative transcriptional activation by retinoic acid receptor and retinoid X receptor. *Mol. Cell. Biol.* **22**, 1446–1459.

50. Kang, Z., Janne, O. A. & Palvimo, J. J. (2004). Co-regulator recruitment and histone modifications in transcriptional regulation by the androgen receptor. *Mol. Endocrinol.* **18**, 2633–2648.

51. Liu, Y., Xia, X., Fondell, J. D. & Yen, P. M. (2006). Thyroid hormone-regulated target genes have distinct patterns of co-activator recruitment and histone acetylation. *Mol. Endocrinol.* **20**, 483–490.

52. Bernstein, B. E., Kamal, M., Lindblad-Toh, K., Bekiranov, S., Bailey, D. K., Huebert, D. J. *et al.* (2005). Genomic maps and comparative analysis of histone modifications in human and mouse. *Cell*, **120**, 169–181.

53. Francis, J., Chakrabarti, S. K., Garmey, J. C. & Mirmira, R. G. (2005). Pdx-1 links histone H3-Lys-4 methylation to RNA polymerase II elongation during activation of insulin transcription. *J. Biol. Chem.* **280**, 36244–36253.

54. Guenther, M. G., Jenner, R. G., Chevalier, B., Nakamura, T., Croce, C. M., Canaani, E. & Young, R. A. (2005). Global and Hox-specific roles for the MLL1 methyltransferase. *Proc. Natl Acad. Sci. USA*, **102**, 8603–8608.

55. Cao, R., Tsukada, Y. & Zhang, Y. (2005). Role of Bmi-1 and Ring1A in H2A ubiquitylation and Hox gene silencing. *Mol. Cell*, **20**, 845–854.

56. Pirrotta, V. (1998). Polycombing the genome: PcG, trxG, and chromatin silencing. *Cell*, **93**, 333–336.

57. Kirmizis, A., Bartley, S. M., Kuzmichev, A., Margueron, R., Reinberg, D., Green, R. & Farnham, P. J. (2004). Silencing of human polycomb target genes is associated with methylation of histone H3 Lys 27. *Genes Dev.* **18**, 1592–1605.

58. Noda, M., Yoon, K., Prince, C. W., Butler, W. T. & Rodan, G. A. (1988). Transcriptional regulation of osteopontin production in rat osteosarcoma cells by type beta transforming growth factor. *J. Biol. Chem.* **263**, 13916–13921.

59. Noda, M., Vogel, R. L., Craig, A. M., Prahl, J., DeLuca, H. F. & Denhardt, D. T. (1990). Identification of a DNA sequence responsible for binding of the 1,25-dihydroxyvitamin D3 receptor and 1,25-dihydroxyvitamin D3 enhancement of mouse secreted phosphoprotein 1 (SPP-1 or osteopontin) gene expression. *Proc. Natl Acad. Sci. USA*, **87**, 9995–9999.

60. Baarends, W. M., Wassenaar, E., van der Laan, R., Hoogerbrugge, J., Sleddens-Linkels, E., Hoeijmakers, J. H. *et al.* (2005). Silencing of unpaired chromatin and histone H2A ubiquitination in mammalian meiosis. *Mol. Cell. Biol.* **25**, 1041–1053.

61. Metzger, E., Wissmann, M., Yin, N., Muller, J. M., Schneider, R., Peters, A. H. *et al.* (2005). LSD1 demethylates repressive histone marks to promote androgen-receptor-dependent transcription. *Nature*, **437**, 436–439.

62. Buchholz, D. R., Paul, B. D. & Shi, Y. B. (2005). Gene-specific changes in promoter occupancy by thyroid hormone receptor during frog metamorphosis. Implications for developmental gene regulation. *J. Biol. Chem.* **280**, 41222–41228.

63. Vaisanen, S., Dunlop, T. W., Sinkkonen, L., Frank, C. & Carlberg, C. (2005). Spatio-temporal activation of chromatin on the human CYP24 gene promoter in the presence of 1alpha,25-dihydroxyvitamin D3. *J. Mol. Biol.* **350**, 65–77.

64. Lefebvre, P., Mouchon, A., Lefebvre, B. & Formstecher, P. (1998). Binding of retinoic acid receptor heterodimers to DNA. A role for histones NH2 termini. *J. Biol. Chem.* **273**, 12288–12295.

65. Boylan, J. F., Lufkin, T., Achkar, C. C., Taneja, R., Chambon, P. & Gudas, L. J. (1995). Targeted disruption of retinoic acid receptor alpha (RAR alpha) and RAR gamma results in receptor-specific alterations in retinoic acid-mediated differentiation and retinoic acid metabolism. *Mol. Cell. Biol.* **15**, 843–851.

66. Reid, G., Hubner, M. R., Metivier, R., Brand, H., Denger, S., Manu, D. *et al.* (2003). Cyclic, proteasome-mediated turnover of unliganded and liganded ER-alpha on responsive promoters is an integral feature of estrogen signaling. *Mol. Cell*, **11**, 695–707.

67. Chen, W., Rogatsky, I. & Garabedian, M. J. (2006). MED14 and MED1 differentially regulate target-specific gene activation by the glucocorticoid receptor. *Mol. Endocrinol.* **20**, 560–572.

68. Wang, Q., Carroll, J. S. & Brown, M. (2005). Spatial and temporal recruitment of androgen receptor and its coactivators involves chromosomal looping and polymerase tracking. *Mol. Cell*, **19**, 631–642.

69. Hallikas, O., Palin, K., Sinjushina, N., Rautiainen, R., Partanen, J., Ukkonen, E. & Taipale, J. (2006). Genome-wide prediction of mammalian enhancers based on analysis of transcription-factor binding affinity. *Cell*, **124**, 47–59.

70. Michelson, A. M. (2002). Deciphering genetic regulatory codes: a challenge for functional genomics. *Proc. Natl Acad. Sci. USA*, **99**, 546–548.

71. Thompson, J. R., Chen, S. W., Ho, L., Langston, A. W. & Gudas, L. J. (1998). An evolutionary conserved element is essential for somite and adjacent mesenchymal expression of the Hoxa1 gene. *Dev. Dyn.* **211**, 97–108.

72. Park, S. W., Li, G., Lin, Y. P., Barrero, M. J., Ge, K., Roeder, R. G. & Wei, L. N. (2005). Thyroid hormone-induced juxtaposition of regulatory elements/factors and chromatin remodeling of Crabp1 dependent on MED1/TRAP220. *Mol. Cell*, **19**, 643–653.

73. Bracken, A. P., Dietrich, N., Pasini, D., Hansen, K. H. & Helin, K. (2006). Genome-wide mapping of Polycomb target genes unravels their roles in cell fate transitions. *Genes Dev.* **20**, 1123–1136.

74. Lee, T. I., Jenner, R. G., Boyer, L. A., Guenther, M. G., Levine, S. S., Kumar, R. M. *et al.* (2006). Control of developmental regulators by polycomb in human embryonic stem cells. *Cell*, **125**, 301–313.

75. Zhuang, Y., Faria, T. N., Chambon, P. & Gudas, L. J.

(2003). Identification and characterization of retinoic acid receptor beta2 target genes in F9 teratocarcinoma cells. *Mol. Cancer Res.* **1**, 619–630.

76. Boyer, L. A., Plath, K., Zeitlinger, J., Brambrink, T., Medeiros, L. A., Lee, T. I. *et al.* (2006). Polycomb complexes repress developmental regulators in murine embryonic stem cells. *Nature*, **441**, 349–353.

77. Tolhuis, B., de Wit, E., Muijrers, I., Teunissen, H., Talhout, W., van Steensel, B. & van Lohuizen, M. (2006). Genome-wide profiling of PRC1 and PRC2 Polycomb chromatin binding in *Drosophila melanogaster*. *Nature Genet.* **38**, 694–699.

78. Bernstein, B. E., Mikkelsen, T. S., Xie, X., Kamal, M., Huebert, D. J., Cuff, J. *et al.* (2006). A bivalent chromatin structure marks key developmental genes in embryonic stem cells. *Cell*, **125**, 315–326.

79. Epping, M. T., Wang, L., Edel, M. J., Carlee, L., Hernandez, M. & Bernards, R. (2005). The human tumor antigen PRAME is a dominant repressor of retinoic acid receptor signaling. *Cell*, **122**, 835–847.

Edited by J. Karn